Design of Electromagnetic Clutch System for Toyota 3L Manual Transmission

By

Dandi Workineh

A Thesis submitted to

Mechanical System and Vehicle Engineering Department

School of Mechanical, Chemical and Materials Engineering

Presented in Partial Fulfillment of the Requirement for the Degree of Master's of Science in Automotive Engineering

Adama Science and Technology University

Adama

Feb, 2019

Design of Electromagnetic Clutch System for Toyota 3L Manual Transmission

By

Dandi Workineh

Advisor: Mekonnen Liben (Asst.Prof.)

A Thesis submitted to

Mechanical System and Vehicle Engineering Department

School of Mechanical, Chemical and Materials Engineering

Presented in Partial Fulfillment of the Requirement for the Degree of Master's of Science in Automotive Engineering

Adama Science and Technology University

Adama

Feb, 2019

Approved by Board Examines

I.	Chair, Department Graduate committee	Signature	Date
	______________________________	____________	_______
II.	Internal Examiner	Signature	Date
	______________________________	____________	_______
III.	External Examiner	Signature	Date
	______________________________	____________	_______
IV.	Advisor	Signature	Date
	Mekonnen Liben (Asst. Prof.)	____________	_______

Candidate Declaration

I, hereby declare that the thesis entitled **“Design of Electromagnetic Clutch System for Toyota 3L Manual Transmission”** submitted in partial fulfillment of the requirements for the award of the degree of Master’s of Science in Automotive Engineering is an authentic record of my own work carried out, under the guidance of **Mekonnen Liben (Asst. Prof.)**, Department of Mechanical System and Vehicle Engineering, Adama Science and Technology University, Ethiopia. The matter embodied in this thesis has not been submitted by me for the award of any other degree or diploma. All relevant resources of information used in this thesis have been duly acknowledged.

Candidate	Date	Signature
Dandi Workineh	_______________	________________

This is to certify that the above statement made by the candidate is correct to the best of my knowledge and belief. This thesis has been submitted for examination with my approval.

Advisor	Date	Signature
Mekonnen Liben (Asst.Prof.)	__________________	_________________

ACKNOWLEDGEMENT

First, I would like to express my greatest gratitude to Almighty God for giving me a chance to complete my thesis with all his blessings. I would like to acknowledge my thesis supervisor, **Mekonnen Liben (Asst. Prof)**. I am very thankful that he supervised my thesis and provided me with the much needed assistance in understanding the thesis. Without his guidance and support, I may not be able to achieve the goals of this thesis.

Very special thanks to all lecturers who had thought me this far and to all friends who gave their support to complete my thesis. Finally, I would also like to thank my parents, for their lifelong encouragement. Without their support and confidence in me, I won't have made until this far.

TABLE OF CONTENTS

CONTENTS PAGE

LIST OF TABLES

LIST OF FIGURES

Figures Page

ACRONYMS

AF	Axial flux
ASTU	Adama science and technology university
AWG	American wire diameter gauge
CBD	Core back Depth
DM	Differential machine
EMCS	Electromagnetic clutch system
EMTC	Electromagnetic torque converter
MR	Magneto rheological
PM	Permanent magnet
PMBEC	Permanent magnet bi-stable electromagnetic clutch
VFRT	Variable frequency rotary transformer

NOMENCLATURES

B	Magnetic field [T]
B_{av}	Average electromagnetic field [T]
B_{max}	Maximum electromagnetic field [T]
B_r	Residual electromagnetic field [T]
B_{sc}	Electromagnetic field in the stator core [T]
C	Mean circumference of coil [mm]
F_m	Electromagnetic force[N]
F_n	Normal force [N]
H_p	Magnetic strength in the air gap [A/m]
I	Current [A]
j_g	Current density in winding [A/mm^2]
K	Diameter ratio
L	Total length of coil [m]
L_r	Axial length of rotor[mm]
L_s	Axial length of stator[mm]
L_{ap}	Axial length of armature plate[mm]
L_{ss}	Axial length of stator slot[mm]
L_{sc}	Axial length of stator core[mm]
L_{pm}	Axial length of permanent magnet[mm]
N	Number of turns
P	Number of pole
R	Resistance of coil[Ohm]
R_f	Effective radius of friction surface[mm]
R_o	Outer radius[mm]
R_i	Inner radius[mm]
S	Effective surface area [mm^2]
g	Air gap length[mm]

ω	Angular velocity [rad/sec]
T_f	Maximum transmission torque [Nm]
V	Voltage [V]
μ	Coefficient of friction
μ_o	Vacuum magnetic permeability
ϕ	Polarizing flux [Weber]

ABSTRACT

Clutch is a device used to connect or disconnect engine torque from the transmission based on the will of the driver. The current friction clutch system has many drawbacks. It requires mechanical force which may cause loose of torque. In addition, the direct contact of mechanical parts increases the possibility of parts failure and mechanical noise. This thesis proposes, new Electromagnetic clutch (EMC) system which replaces the current friction clutch system. To achieve the goal of the thesis theoretical design case and analytical method were used. Analytical modeling method were preliminary used to obtain the basic electromagnetic constraints such as; normal force, electromagnetic field density, electromagnetic field strength, length of the air gaps and total number of turns. These parameters are then used to predict geometric dimension and behavior of the complete EMC system. Some stator topology and winding types are compared for use as the EMC system and the parameters that influence them are discussed. Then, topology of the EMC system ware defined and component designs were carried out. Analytical calculation result, showed good agreement with the effectiveness of the EMC system. Finally, the most outstanding conclusion about the EMC system was captured.

Key words: Rotor; Stator; Armature plate; Permanent magnet; optimal design

CHAPTER ONE

1. INTRODUCTION

1.1 Background of the Study

Automotive industry is changing every day. Billions of dollars are invested in research and development for building safer, cheaper and better performing vehicles. One such investment is the "electromechanical "topic which has been introduced to improve the existing mechanical systems on automobiles. Mechanical systems in the vehicles can be replaced by electromechanical systems that are able to do the same task in a faster, more reliable and accurate way than the pure mechanical systems. This thesis work is concerned with the topic of electromagnetic clutching in vehicles. Nowadays, conventional friction clutch is being used by many late model vehicles including Toyota 3L, manual transmission. This system involves the clutch pedal, hydraulic fluid, transfer pipes and clutch actuators (pressure plate, clutch disk and diaphragm springs). These clutches are mechanical subsystems of the power-train. For intermittent periods only, the transmission of rotary motion from one shaft to another is achieved by this clutch. Then, this coupling must be maintained for transmitting the entire mechanical power from the driving shaft to the driven shaft without subsequent slip (Bezzazi, Khamlichi et al. 2006). However, the friction clutch has a number of disadvantages. The internal piston seals on the master and slave cylinder can develop leaks that allow a loss of pressure when the clutch pedal is depressed. This may prevent the clutch from disengaging or allow it to slip. The basic hydraulic linkage of the friction clutch is shown in figure 1.1.below.

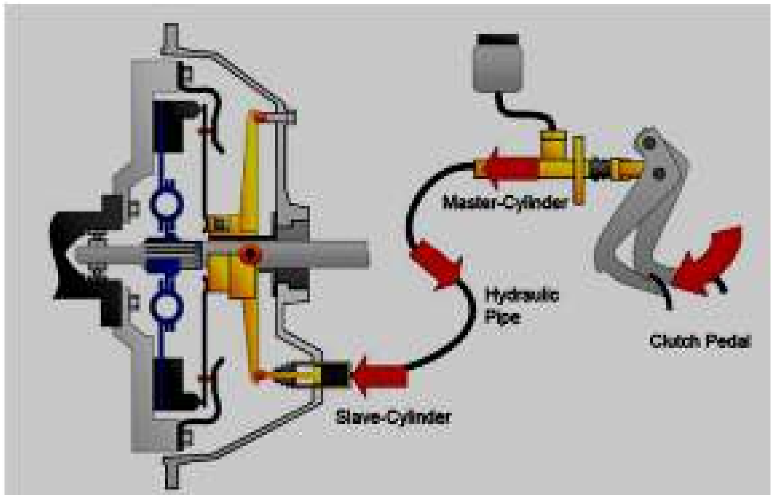

Figure 1.1: Hydraulic Clutch Linkage (www.autopartslib.com).

However, with the introduction of electromechanical technologies, electromagnetic clutches (EMC) have appeared in some machines. Electromagnetic clutches are equipment drive assemblies that contain electrically actuated components for connecting two shafts so that they can either be locked together and spin at the same speed, or decoupled and spin at different speeds. Engaging the clutch transfers power from driving shaft to driven (output) shaft. Disengaging the clutch stops the power transfer, but allows the driving shaft to continue turning. Electromagnetic clutches are already used in several systems in today's world. You can find them in lawnmowers, copy machines, compressors and even some automobiles air conditioning system (Samuel, 2006). My concern is to design this equipment's for Toyota 3L manual transmission clutch system applications.

1.2. Problem Statement

The current friction clutch system of Toyota 3L manual transmission has many drawbacks which have significant impact on engine output torque, proper operation of the clutch system and driver comfort. The clutch system uses the friction disc between flywheel and the pressure plate as its coupling mechanism. Due to the friction disc wear and the friction coefficient variation in friction material, the clutch performs less optimally with the increased number of usage cycles. Thus, the friction disc must be changed periodically in order to get the optimum clutch performance which raises the price of maintenance. Another problem of the clutch system includes: Oil leakage, Excessive slippage, diaphragm spring wear and flywheels face run out (Lathiya, Badola et al. 2014). This thesis proposes, new Electromagnetic clutch (EMC) system which replaces the current friction clutch system. The advantage to this concept is that torque is transmitted magnetically; there is no direct contact of mechanical parts. Thus the proposed EMC system is expected to be solution for the problem of the current clutch system.

1.3 Objectives of the Study

1.3.1 General Objective

The general objective of this thesis is to design electromagnetic clutch system for Toyota 3L, Manual transmission.

1.3.2 Specific Objectives

To attain the above general objective, the study focuses on achieving the following specific objectives:

- ✓ Analysis of failure and factors that affect the current friction clutch torque.
- ✓ Develop preliminary design of the EMC system.
- ✓ Mathematical modeling and analytical optimization of electromagnetic circuit constraints and geometric dimensions of the EMC system.
- ✓ Component design for the EMC system.
- ✓ Evaluate performance of the EMC system relative to the existing clutch system.

1.4 Scope of the study

The motivation behind this thesis is the need of electromagnetic clutching devices for manual transmission that yield low loses and parts failure while matching performance of the existing clutch system. Investigation on the physical principles governing the operation of electromagnetic clutch actuated technology is undertaken. These principles then lead to generation of new design concept and needs to dedicate for Toyota 3L, manual transmission. Therefore, based on the available time, the thesis work was limited to mathematical modeling, numerical calculation and 3D modeling of the EMC system by using CAD software.

1.5 Significance of the Study

The beneficiary of the thesis work are; the automotive industry in particular, the researcher, vehicle owners, drivers, and the country when the outcome from the thesis becomes evaluated and implemented. The following are the extent to which the proposed thesis work is important.

- ✓ Saving cost of fuel.
- ✓ Saving currency invested for import of clutch spare parts.
- ✓ Minimized clutch power loss.
- ✓ Improve safety of the driver.

1.6 Arrangement of the thesis

This thesis consists of five chapters.

Chapter-1 Fully describes the problems of the existing friction clutch system in light of its performance capability. The problem of the statement, Objectives, scope and significance of the study is well explained.

Chapter-2 Focused on a literature review surrounding the subject of this thesis work. The friction clutch model, analysis of failure and factors that affect the friction clutch torque are explained. Then developments on clutch technology with electromagnetic clutch system are mentioned. Electromagnetic clutch actuated technology and a basic design concept of electromagnetic clutch are presented. Finally, explain research landscape and the research gap identified.

Chapter-3 Describe the Materials and methods used in this thesis work. Data collection and analysis method, design procedure and flow chart of work necessary for the thesis are elaborated. Preliminary design and mathematical modeling of the EMC system are described. Analytical method was applied and the electromagnetic properties of the EMC system are determined. Finally, component design and 3D modeling of the EMC system is carried out by using CAD software.

Chapter-4 Explain results and discussion with the major problems of the existing clutch system. The design ideas, analytical calculation result and advantage of the EMC system are presented in detail. Summary of the multi disciplinary design and analysis method used for the thesis work is explained.

Chapter-5 summarizes the main results and conclusions of the thesis and recommendation for the future work direction.

CHAPTER TWO

2. LITERATURE REVIEW

2.1 Introduction

The following section reviews the state of research surrounding the subject of this thesis, the design of Electromagnetic clutch system for Toyota 3L, manual transmission. The increased global focus on high efficiency clutch systems is discussed, specifically in the context of manual transmission. Different problems of friction clutches are explained. Developments of friction clutches are discussed; with a review of Electromagnetic clutch systems actuated technologies.

2.2 The friction clutch

A Clutch is an important part in the transmission system of automobiles. It transmits power from the engine to gear box at various speeds. The most common type of commercial clutch is the friction clutch, such as those used in Toyota 3L, manual transmissions. The friction clutch works on the principles of friction. When two friction surfaces are brought in contact with each other and pressed they are united due to the friction between them. If the driving part rotates the driven part also rotates. The two surfaces can be separated and brought into contact when required. The driving member is rotating as the car engine starts to run; when the driven member is brought in contact with the driving member, it also starts rotating. When the driven member is separated from the driving member it does not rotate. The friction between the two surfaces depends upon the area of the surfaces, pressure applied upon them and co-efficient of friction of the surface materials. In a friction clutch, the input is in physical contact with the output via a normal force applied by some actuating mechanism. This normal force is generated hydraulically. The friction between the two contacting surfaces, applied at a distance from the rotation axis, transmits torque. Figure 2.1 illustrates this, friction clutch configuration (Lathiya, Badola et al .2014).

Figure 2.1: Components of the friction clutch

2.2.1. The friction clutch model

A friction clutch model is shown in Figure 2.2. It is obvious that the torque on the driving shaft must exactly equal to the torque on the output shaft. In fact, these two torque are actually one and the same torque, because the torque is caused by friction between the discs and it is true whether the clutch is slipping or not. Let ω_1 and ω_2 be the angular velocities of the shaft when the clutch is slipping.

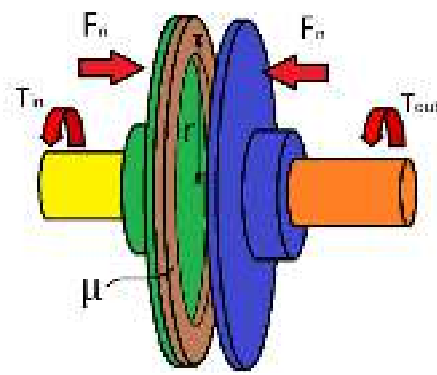

Figure 2.2: Friction disk clutch model (Jessy cussack, 2013)

The torque transmitted via friction clutch is given by:

$$T_f = \mu \times Rf \times Fn \quad (2.1)$$

Where,

T_f	Torque transmitted via friction [Nm]
R	Effective radius of friction surface [mm]
F_n	Normal force applied to friction surface [N]
μ	Co efficient of friction

Towards the goal of maximizing torque, all three terms on the right side of the equation 2.1 should be maximized. In practice, high friction composites are used to maximize μ, and R is maximized within packaging allowances of the application. Torque capacity is then limited only to the amount of normal force that can be applied. The engagement and disengagement speed of a friction clutch is dependent on its actuation method. However, normal force that can be applied to engage the friction clutch is not constant and it decreases with friction disc wear which results in clutch slip and power loose. No commercially available friction clutches meet the constant actuation force and speed demands of clutch system. This is identified as a gap in current technology. With Electromagnetic clutch actuation mechanism employed, torque transfer via EMCS has the potential for constant normal force application aspects, slip and wears problem reduction (Jessy cussack, 2013).

2.2.2 The influence of contact properties of friction clutch

The real area of contact is only a small percentage of the nominal surface area (GAO and Barber, 2002). This contact area can be calculated by capturing grey-scale images, and then converting them into binary images, where the perimeters of the contact area can be traced. This real contact area increases with the contact pressure, as more fibers deform and wear. It is also observed that the shear strength of the boundary film has a strong dependency on the contact area (Eguchi and Yamamoto, 2005). During the operation of a friction material it will wear, which can affect the performance of the clutch. Wear occurs on the uppermost regions of the friction material during sliding, as material is lost from the fibers by adhesive, abrasive and ploughing wear. The outer resin layer will probably be lost in the first instance, but the inner cellulose fibers and regions of filler materials may also be lost, as the wear of the material continues. The removal of material in this way will cause the formation of smooth, flat areas on the uppermost regions of the contact units, parallel to the direction of sliding, leading to the formation of larger contact units. The larger units will make the material less rough and hydrodynamic films may form between them and the steel surface, leading to a reduction of friction and poor clutch performance. The removal of material will also change the surface chemistry of the material, as the outer resin layer is removed, the inner cellulose or filler material, may be exposed. The wear of the friction material and its effect on the real area of contact has been studied experimentally by (Sanda, 1995).

Namrata and Prof.Dheeraj.V (2016) has analyzed 23^o Inclined Grooves Made on Dry Friction Clutch**.** Mostly here we have used friction clutches and has transmit the torque from one shaft to another shaft at that time huge amount of energy have been induced in it and results in wear. The slipping clutch mechanism generates heat energy due to friction between flywheel and the clutch disc. Excessive frictional heat is generated at high sliding velocity which lead to causes thermo-mechanical problems because of high temperature rise the clutch disc surface such as thermal deformations and thermo-elastic instability occurs which lead to thermal cracks, wear and other mode of failure of the clutch disc component. Hence for getting the results we have done here the analysis of the 23^o inclined grooves made on the dry friction clutch plate in the ANSYS by taking the reference of Maruti alto 800.

Cappetti, Marion et al. (2012) factor that directly affects the clutch torque is the clamp load. The clamp load is dependent on the actuator position. These characteristics are reported to have a decreasing with disc wear.

Poturi, Cusak et al. (2003) has analyzed the parts of a single plate clutch. It has only one clutch plate, mounted on the splines of the clutch shaft. This is the most commonly used type. The axial movement of the pressure plate is effected by pressing the clutch pedal. After researching and studying on this clutch, it was found that during its operating condition, it takes some time for alignment and wear occurs during alignment.

Lathiya, Badola et al. (2014) reviewed a literature on Failure in Single Plate Clutch System. The clutch engages the transmission gradually by allowing a certain amount of slippage between the flywheel and the transmission input shaft. However, the slipping mechanism of the clutch generates heat energy due to friction between the clutch disc and the flywheel. At high sliding velocity, excessive frictional heat is generated which lead to high temperature rise at the clutch disc surface, and this causes thermo-mechanical problems such as thermal deformations and thermo-elastic instability which can lead to thermal cracking, wear and other mode of failure of the clutch disc component.

Ravibala, Dr.SS.Chauhan et al. (2016) has reviewed friction clutch plate. In this thesis static and thermal analysis is done to find the temperature variation and heat flux of the friction plate. By observing the analysis results, the stress values are more for composite materials and when the crack is started the composite materials, stress values increases more than the condition of no crack so the composite materials fails faster once the crack propagates. And it is found that the temperature developed during the engagement and disengagement process is beyond the maximum temperature of the gray cast iron material. i.e. there is crack and erosion of the friction material of the friction plate that the values of temperature increase linearly with disc radius and the maximum temperature.

2.2.3. Influence of friction clutch pedal to ride comfort

Jiangchuan, Fung et al. (2013) has analyzed the Influence of Clutch Pedal to Vehicle Comfort. Clutch pedal force and pedal motion stroke mainly affect the driving comfort. Too light pedal force makes drivers feel the juncture not obviously, too heavy pedal force makes drivers fatigue; if the separation distance was too short, there would be flameout problem if the combined distance is too long and this may also make drivers feel pedal engagement point is much more higher. Pedal force and pedal motion stroke are the main factors influencing clutch manipulation.

2.3. Electromagnetic clutch

Electromagnetic clutches are equipment drive assemblies that contain electrically actuated components for connecting two shafts so that they can either be locked together and spin at the same speed, or decoupled and spin at different speeds. Engaging the clutch transfers power from driving shaft to output shaft. Disengaging the clutch stops the power transfer, but allows the driving shaft to continue turning. Electromagnetic clutches operate electrically but transmit torque mechanically. When Electromagnetic clutch is actuated, current flows through the electromagnetic coil producing a magnetic field. The rotor portion of clutch becomes magnetized and sets up a magnetic loop that attracts the armature. When current is removed from EMCS, the armature is free to rotate the driven shaft (Athani, Rama et al. May 2016).

2.3.1. Constructions of Electromagnetic Clutch system

The electromagnetic clutch consists a stator body contains the field coil, rotor and armature. The clutch is activated by applying a direct current to the field coil. This creates a magnetic field, which electromagnetically attracts the armature towards the rotor and so allows torque to be transmitted from the rotor to the armature. The followings are the main component in the electromagnetic clutches.

i. **Stator body and field coil**: - It is the one of the most important part in electromagnetic clutch. The coil is wound in the stator body. The current to the coil is delivered from the battery and the north and South Pole is created by this coil.

ii. **Rotor**: - Is the rotating member whose magnetic field couple with stationery magnetic fields of the stator to attract the armature disc and drive load.

iii. **Armature: -** When the coil is energized, the armature plate is attracted to the rotor with substantial magnetic force, allowing torque to be transmitted from the rotor to output shaft (Bodine hand book, 2001).

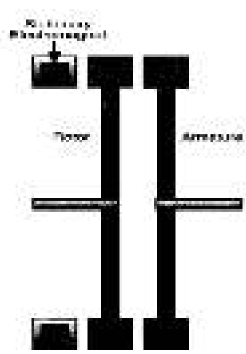

Fig 2.3: Configuration of EMC (Bodine hand book, 2001).

2.4. Electromagnetic actuator technologies

Of a various electromechanical linear actuators, electromagnetic actuators have drawn special attention. Electromagnetic actuators use magnetic fields to generate forces which lead to motion. In an electromagnetic actuation system, the input electrical energy in the form of a voltage and a current is converted to magnetic energy. The magnetic energy creates a magnetic force which produces mechanical motion over a limited range. Typically, the magnetic force is generated due to the magnetic field interaction built by the current-carrying coil or the permanent magnet. Thus, magnetic actuators convert input electrical energy into output mechanical energy as shown in Figure 2.3. Further, electromagnetic actuators typically offer strokes in the range of 1 to 20 mm. Moreover, due to the rapid development and disappearance of magnetic energy in the magnetic fields, electromagnetic actuators demonstrate very fast operation speeds.

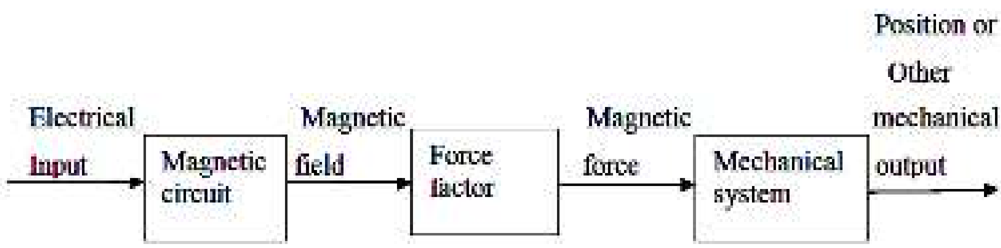

Figure 2.4: Block diagram of the electromagnetic actuator (Vahid Mashatan, 2013).

Compared with pure hydraulic, electro-hydraulic, electromechanical, and piezoelectric actuation technologies, electromagnetic actuation technology is simpler, cheaper, more repairable, robust, and more manufacture able. Particularly, advantages of electromagnetic actuation technology are as follows:

- ✓ High actuation force
- ✓ Long stroke (displacement)
- ✓ Fast response
- ✓ Contactless remote actuation
- ✓ Low voltage actuation

- ✓ Bi-directional actuation
- ✓ Design flexibility
- ✓ Potentially high energy density

In order to analyze the electromagnetic actuators it is important to understand the governing principle for these actuators. The electromechanical conversion mechanisms in electromagnetic actuators are governed by the Lorentz force law and Reluctance force law (Vahid Mashatan, 2013).

Lorentz Force Law states that if a current-carrying conductor is placed in a magnetic field, a force will act upon it. The magnitude of this force is determined by the magnetic flux density, the current, and the length of the conductor placed in the magnetic field. The Lorentz force is proportional to the product of the magnetic field and the current, in a direction perpendicular to both of them as shown in Figure 2.4. By reversing the polarity of the voltage in the conductor, the direction of the force will change (Bodine handbook, 2001).

Reluctance force Law states that for a current carrying conductor in a stationary coil, the electromagnetic system always tries to move toward the status of minimum reluctance in its magnetic circuits. Therefore, if any part of the magnetic circuit is free to move like a plunger in a solenoid, a force is generated which causes the plunger to move in order to minimize the magnetic reluctance of the magnetic circuits. The generated pulling force is proportional to the square of the current in the windings and inversely proportional to the square of the length of the air gap (Bodine hand book, 2001).

2.5. Development of clutch technology with the Electromagnetic clutch

There have been many attempts to develop the performance of the clutch system to improve reliability and provide greater efficiency. The background of the Electromagnetic clutch system currently available is given below.

Martin, Steinberg et al. (2015) in this paper friction clutch capable with an electromagnetic actuator has considered. The goal of author is to estimate the air gap between an electromagnet and an armature, which allows compressing the clutch discs. In order to advance the estimation, a sliding mode observer using super twisting concepts is developed.

Rico.B (2012) have developed electromagnetic clutch for automotive air conditioning system. In this electromagnetic clutch system, when the air conditioning is activated, the electromagnetic coil is supplied with power, which pushes the carrier disk onto the pulley. As a result, a friction force develops between the pulley and the friction pads on the carrier disk. Thus the carrier disk and the compressor shaft are driven. When the compressor shaft reaches a particular rotational speed, the centrifugal force might move the locking elements outwards in radial direction. If the locking elements immediately snapped into the grooves that are integrated in the pulley ring, the clutch could be damaged because of the speed difference between the carrier disk and the pulley. To avoid this, an edge in the pulley keeps the locking elements from engaging with the grooves.

Jiang, Heren et al. (2015) has analyzed on application and control method of electromagnetic synchronizer with power coupling system of double rotor motor. It aims in adding electromagnetic coupling between the two shafts as enhancement in transmission system. Electromagnetic synchronizer voltage for driver is controlled through PID.

Eljaroshi .E (2014) has designed electromagnetic torque converter (EMTC). This thesis proposes a new and novel Electromagnetic Torque Converter system, which replaces the conventional hydraulic torque converter. The new EMTC system comprises of two parts, a Differential Machine (DM) part, which is a double rotor single stator machine, and a Variable Frequency Rotary Transformer (VFRT) part, which is responsible for transferring the slip power from between the DM rotors to the DM stator. The new EMTC system resolves many of the drawbacks of the conventional hydraulic torque converter.

Wanli (2015) worked on Analysis and design of permanent magnet bi-stable electromagnetic clutch unit for in wheel electric vehicle drives. This paper proposes a permanent magnet bi-stable electromagnetic clutch unit (PMBECU), which is controlled by current and held by the PM (permanent magnet) in a steady state, and thus is energy-saving, and it also has a flat structure that makes its placement in a limited space viable. The influence of the temperature on the dynamic performance is also analyzed.

Kirchengast (2015) they have studied for electromagnetic clutches can be used to transmit a continuously adjustable torque from the main shaft to the budge shaft. In contrast to friction clutches, electromagnetic clutches transmit rotation by a magneto-rheological fluid consisting of a base fluid mixed with numerous Ferro-magnetic micro-sized particles. Once the flux density is increased, the micro-sized particles start to form firmly tied chains increasing transmitted torque. The results show that the designer can obtain different models depending on the formulation of the objective function.

Francesco, Paola et al. (2015) this article gives the torque characteristic of a permanent magnet magneto rheological (MR) clutch is investigated focusing on the influence of temperature. In particular, a loss of transmitted torque for increasing temperature was found. An Approximate dependence of MR fluid shear stress on temperature, useful for similar devices, was also obtained. In this paper work, the effects of temperature on the torque transmission characteristics of an MR were experimentally investigated.

Erickson (2001) has proposed Fundamentals of power electronics. A novel means of approaching flywheel energy transmission is through Switch-mode control. Switch-mode systems have long been in use in electrical engineering, where circuits may switch between two or more discrete states to improve functionality and efficiency for tasks such as power transfer. As the most basic properties of electronic components– capacitance, resistance, and inductance – are analogous to those of mechanical systems – stiffness, damping, and inertia – inspiration for mechanical systems may be drawn from electronic power solutions. As an example, one of the most basic switch-mode circuits used for power transfer is the DC boost converter, a type of regulated power supply.

Jaindl.M (2015) they have studied for electromagnetic clutches can be used to transmit a continuously adjustable torque from the main shaft to the budge shaft. In contrast to friction clutches, electromagnetic clutches transmit rotation by a magneto-rheological fluid consisting of a base fluid mixed with numerous Ferro-magnetic micro-sized particles. Once the flux density is increased, the micro-sized particles start to form firmly tied chains increasing transmitted torque. The magnitude of the torque can be regulated by the application of an appropriate magnetic field which is simulated by the Finite-Element-

Method. The results show that the designer can obtain different models depending on the formulation of the objective function.

M. Montanari (2012), in this paper hydraulic actuated clutch control system for commercial cars is analyzed. The design of closed-loop controller is presented, based on a simplified system model. A physical full-order model is also described and used to assess through computer simulations the dependence of the closed-loop system performances on some plant and controller key parameters. Investigational tests performed with different plant and controller configurations are reported. They closely match the simulation results, showing the effectiveness of the proposed approach.

2.6. Basic design concepts of Electromagnetic Clutch system

2.6.1 Electromagnetism

When current passes through a conductor, magnetic field will be generated around the conductor and the conductor become a magnet. This phenomenon is called electromagnetism (Jack Erjavec, 2009).

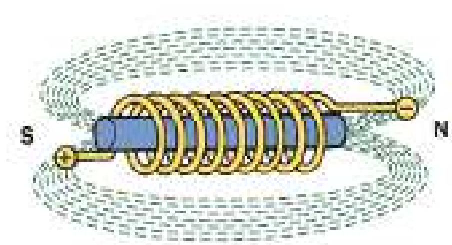

Figure2. 5:-Electromagnetism (Jack Erjavec, 2009)

The direction of the magnetic field formed by a current carrying straight wire can be determined by the Right Hand Grip Rule or the Maxwell Screw Rule.

Right hand grip rule- Grip the wire with the right hand, with the thumb pointing along the direction of the current. The other fingers give the direction of the magnetic field around the wire (Bodine hand book, 2001).

Maxwell Screw Rule- the Maxwell Screw Rules sometime is also called the Maxwell's Corkscrew Rule. Imagine a right handed screw being turn so that it bores its way in the direction of the current in the wire. The direction of rotation gives the direction of the magnetic field (Bodine hand book, 2001).

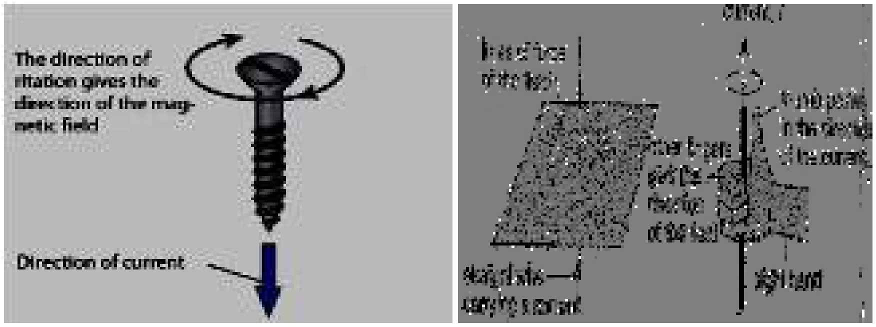

Figure2. 6:-A. Maxwell Screw Rule B. Right hand grip rule

Whenever a current-carrying conductor is placed in magnetic field, it experiences a force which acts in a direction perpendicular both to the direction of the current and the field. The force on the current carrying conductor in a magnetic field depends on:-

i. The flux density of the field (B).
ii. The strength of current (I).
iii. The length of the conductor perpendicular to the magnetic field.
iv. The direction of the field and current.

When the magnetic field, the current and the conductor are mutually perpendicular to each other then force exerted is given as (B.L.Theraja, 2005):

$$F = I \times B \times L \qquad (2.2)$$

When the conductor and magnetic field are at an angle, then the force exerted is given as (B.L.Theraja, 2005):

$$F = I \times B \times L \times \sin \alpha \qquad (2.3)$$

Where,

F	Electromagnetic force [N]
B	Electromagnetic field [Tesla]

2.6.2.	L	Length of conductor [mm]
	Sinα	Angle between conductor and magnetic field [Deg]

Electromagnet

An electric current can be used for making temporary magnets known as electromagnets. An Electromagnet works on the magnetic effect of current. It has been found that if a soft iron rod called core is placed inside a solenoid, then the strength of the magnetic field becomes very large because the iron ore is magnetized by induction (Prof.R.P.Kattimani et.al, 2018).

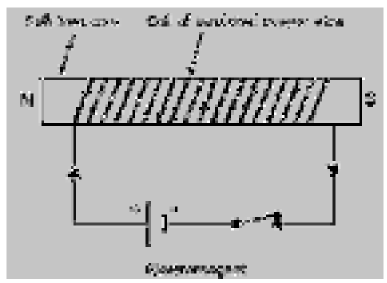

Figure 2.7: Magnetic field lines (Prof.R.P.Kattimani et.al, 2018).

When a piece of iron is attracted by a magnet, it also temporarily becomes a magnet, and a series of pieces of iron will attract one another successively so long as the first piece is influenced by the magnet. This phenomenon is said to be the result of Magnetic Induction. In this case the pieces of iron tend to form a good con ducting path for the lines of force; hence, the more perfectly they tend to close the magnetic circuit, the greater will be their attraction for one another (Charles, 2010). The property of a material which opposes the creation of magnetic flux is known as reluctance. It measures the opposition offered to the passage of magnetic flux through a material and is analogous to resistance in an electric circuit even in form. In other words, the reluctance of a magnetic circuit is the number of amp-turns required per Weber of magnetic flux in the circuit (B.L.Theraja, 2005).

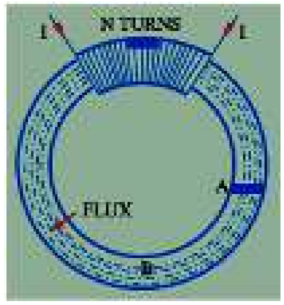

Figure 2.8: Magnetic circuit (B.L.Theraja, 2005).

2.7. Design parameters of friction clutch system

The torque transmitted by friction clutch system is related to the actuating force, the coefficient of friction, and the geometry of the clutch. In analyzing the performance of the friction clutch we shall be interested in:

- ✓ The actuating force
- ✓ The torque transmitted
- ✓ The energy loss and the temperature rise (Dr.Haftirman, 2015).

2.8. Stress analysis of friction clutch system

The normal force is assumed to be uniformly distributed over the effective area of the clutch and attempts to pull the clutch apart. Its effect is similar to those caused by an internally pressurized cylinder and what cause failure in the clutch is typically the tangential stress. The maximum stress that the clutch must handle is tensile strength. By considering uniform pressure theory intensity of the tangential stress can be defined by using the following equation (Gupta, 2005).

$$\sigma_t = \frac{F_n}{A} \qquad (2.4)$$

Where,

σ_t	Tangential stress [N/m^2]
F_n	Normal force [N]
A	Effective area of the clutch [m^2]

In addition to the tangential stresses, centrifugal stress due to rotation of the clutch system contributes to the loading of the clutch. The rotational stress level on the clutch can be calculated by the following equation (P.Kattimani, 2018).

$$\sigma_t = \rho \times \omega^2 \times R^2 \qquad (2.5)$$

Where,

ω	Angular velocity [rad/sec]
ρ	Density of the material [Kg/m^3]
R	Outer radius of the clutch [m]

2.9. Research landscape

Several automotive researchers have focused on the development of friction disc material and electromechanical systems in power trains. Different types of electronic controlled clutches have been developed in the past (Erickson, 2001).There is primarily two classes of electromagnetic controlled clutches, i.e. friction clutches and contactless clutches. The frictional electromagnetic clutches are based on the principle of the mechanical disc and electromagnetic actuation of engagement (Martin, Steinberg et al .2015). However, the contactless clutches are based on electro magnetized driving part designs with driven part arrangements (Rico, et.al, 2012), (Wanli, 2015), (Eljaroshi, 2014) electromagnetic synchronizer with power coupling system (Jiang et al, 2015) and is the subject of this paper. Electromechanical systems boast several benefits such as compactness, simple controls, fast response and reliability. These systems have been used, for example, in air conditioning systems (Rico, et.al 2012). Furthermore, some researchers have also explored electromagnetic torque converter system, which replaces the conventional hydraulic torque converter (EMTC) .The new EMTC system resolves many of the drawbacks of the conventional hydraulic torque converter. (Eljaroshi, 2014).

2.10. Research gap

According to the literature reviewed regarding the current friction clutch system and its related problem, different issues are addressed. Several electromagnetic torque transfer concepts are reviewed. Electromagnetic clutch control is identified as an ill-explored area of thesis work. Electromagnetic clutch system is not used in manual transmission car yet. Finally, from what observed and reviewed from books, journals, magazines and other sources, gap observed, combined together and gives the topic of the thesis as 'Design of Electromagnetic Clutch system for Toyota 3L, Manual Transmission.' This project will make an impressing mark in the field of automobile. The conventional clutch system has a lot of problems like oil leakage, difficulty of operation, complex linkage, wear and slip. But the proposed EMCS has no physical contact between driving and driven part. Therefore, it is an effective method of improving the current friction clutch power loose and failure problem.

CHAPTER THREE

3. MATERIALS AND METHODS

3.1. Introduction

This chapter provides three categories namely, the methodology of the EMC system design along with the data collection and analysis methods, Preliminary design and design optimization of the proposed EMC system.

3.2. Methods

This section presents and explains the methodology in this thesis work. At starting point of the thesis work the conventional clutch system was explained in light of its problem. The up to date techniques in developing the conventional clutch system was investigated. The investigation showed that, EMC technique has not been used for manual transmission car. In manual transmission car, friction clutch system couples engine with the gearbox at all times using the friction disc, pressure plate and diaphragm spring. Therefore, the philosophy behind this thesis work is to perform this coupling by using electromagnet rather than by friction disc, pressure plate and diaphragm spring. The use of an electric machine instead of mechanical coupling is desirable due to the high efficiency of electric machines, especially the permanent magnet machines. In addition, the speed response of electric machines is faster than the mechanical coupling (Eljaroshi, 2014).This thesis work will focus on design of Electromagnetic clutch system suitable for Toyota 3L manual transmission. The

Electromagnetic clutch system consists of rotor, stationery electromagnet (stator) and armature plate. Analytical optimization method is used to achieve electromagnetic circuit constraints and geometric dimensions of the proposed electromagnetic clutch system.

3.3. Design procedure

Previous studies, journal papers and online articles are reviewed for the design of EMCS. This provides evidence of familiarity with the areas covered in this thesis work. Six stages are adopted to achieve the thesis aim. A summary of the stages used in design procedure of this thesis work is given below.

Stage 1 Data collection and analysis. At this stage main dimensions of clutch and specifications of Toyota 3L manual transmission are identified.

Stage 2 Configuration of the proposed EMCS with its working principle. At this stage, mathematical modeling and sizing equations for the electromagnetic circuit are carried out.

Stage 3 Design and optimization of the electromagnetic circuit parameters. At this stage preliminary design was developed. The normal force, effective cross sectional area and effective radius of the proposed EMC system are defined. These values are then used as an input to calculate the magnitude of electromagnetic circuit constraints. Then the EMC system design limitations are defined.

Stage 4 Comparison and selection of stator topology and stator winding type suitable for the design of the proposed EMC system.

Stage 5 Establish topology of the whole EMC system. At this stage set of design ideas and sizing equations are carried out. Axial dimensions of the EMC components are defined.

Stage 6 Component designs for the proposed EMC system. At this stage geometric dimension and 3D modeling of the components has been defined by using CAD soft ware. Figure 3.1 shows flow chart of design procedure for the EMC system.

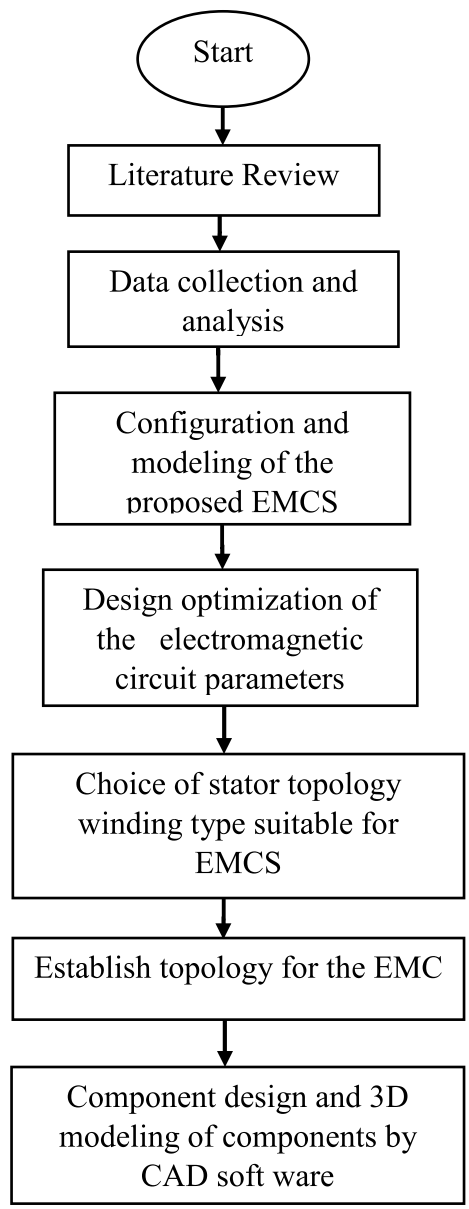
Start
Literature Review
Data collection and analysis
Configuration and modeling of the proposed EMCS
Design optimization of the electromagnetic circuit parameters
Choice of stator topology winding type suitable for EMCS
Establish topology for the EMC
Component design and 3D modeling of components by CAD soft ware

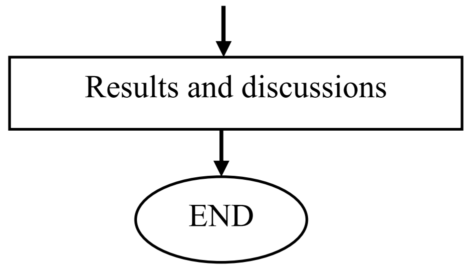

Figure 3.1: Flowcharts of the strategy of the EMC system design

3.3.1. Data collection and analysis method

In this thesis work both primary and secondary information source are used. The secondary data are gathered by measuring the main clutch dimensions of Toyota 3L, manual transmission which is available in the ASTU automotive workshop. Fig.3.2 shows main dimensions of the clutch system.

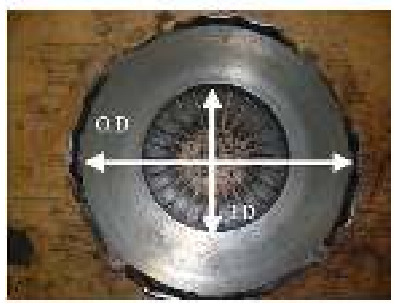

Figure 3.2: Toyota 3L, clutch main dimension

The main dimensions of the clutch are measured by using vernier caliper and the values are given below:

- ✓ Outer diameter of pressure plate =275mm.
- ✓ Inner diameter of the pressure plate =175mm
- ✓ Axial length of bell house =200mm

The primary data are collected from manual of the car and the results from the analytical calculations are used for initial start of the thesis work. Figure 3.3 shows Toyota 3L, manual transmission.

Figure 3.3: Toyota 3L, manual transmission

The car engine was only capable of delivering a gross mechanical power of 68kW (91hp) at 4800rpm and peak torque of 180Nm (Toyota 3L manual, 2001). The primary and secondary data listed in Table 3.2 are the design requirements of the proposed electromagnetic clutch system.

Table 3.1: Clutch and engine Specification of Toyota 3L, manual transmission.

No	Parameters	Values	SI	Remark
1	Peak torque output (T)	180	Nm	Toyota 3l Manual ,2001
2	Peak power(P)	68	KW	Toyota 3l Manual ,2001
3	Diameter of flywheel	280	mm	Measured
4	Coefficient of friction for friction disc	0.2	-	Toyota 3l Manual ,2001
5	Axial length of bell house	200	mm	Measured
6	Outer diameter of pressure plate (d_O)	275	mm	measured
7	Inner diameter of pressure plate (d_i)	175	mm	measured

Note: The new proposed EMCS should meet the specification and volume provided for conventional clutch system of Toyota 3L, manual transmission listed in table 3.2.Engine specification and clutch volume is limited parameters. However, the normal force required to hold the clutch in engaged position can be calculated from engine output torque. The result from analytical calculation is used as an input for the design of the proposed EMC system. The electromagnetic field generated would be capable of coupling the input and output components of the proposed EMC assembly for the given engine torque of 180Nm.

3.4. The proposed Electromagnetic Clutch system concept

The proposed Electromagnetic clutch (EMC) system is designed to be integrated into a Toyota 3L, manual transmission. The bell house of the car is assumed to enclose the EMC system. With no requirement of clutch diaphragm spring, pressure plate, friction disc or a hydraulic linkage, the number of clutch component is significantly reduced. The EMC system has three main parts: rotor, stator and armature plate. The rotor is normally connected to the part that is always moving with the engine. The armature plate is connected to the component that requires the acceleration. The stator is sandwiched between rotor and armature plate. The whole structure of the EMC system is shown in Figure 3.4.below.

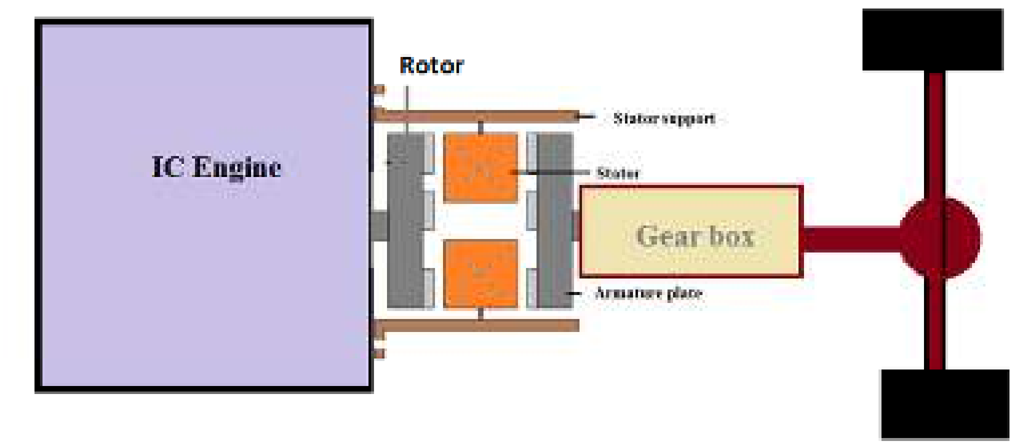

Figure 3.4: Configurations of the proposed EMC system.

3.4.1 The Electromagnetic Clutch system description

The clutch is activated by applying a direct current to the stator coil. This creates a magnetic field, which electromagnetically couple the rotor with armature plate and so allows torque to be transmitted from the rotor to the armature plate as shown in figure 3.5.

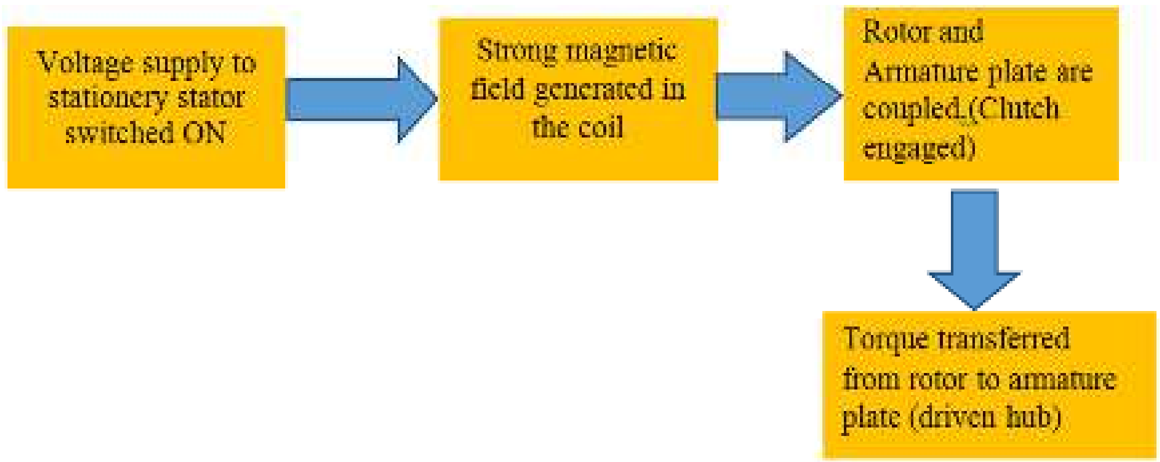

Figure 3.5: Flow charts of EMC system engagement.

Disengagement is very simple. Once the field starts to degrade, flux falls rapidly so the rotor and armature plate decouple. The gear lever consists of a clutch release switch. When the driver holds the gear lever to change the gear, the switch is operated cutting off the current to the stator winding which causes the EMC system disengaged as shown in figure 3.6 below.

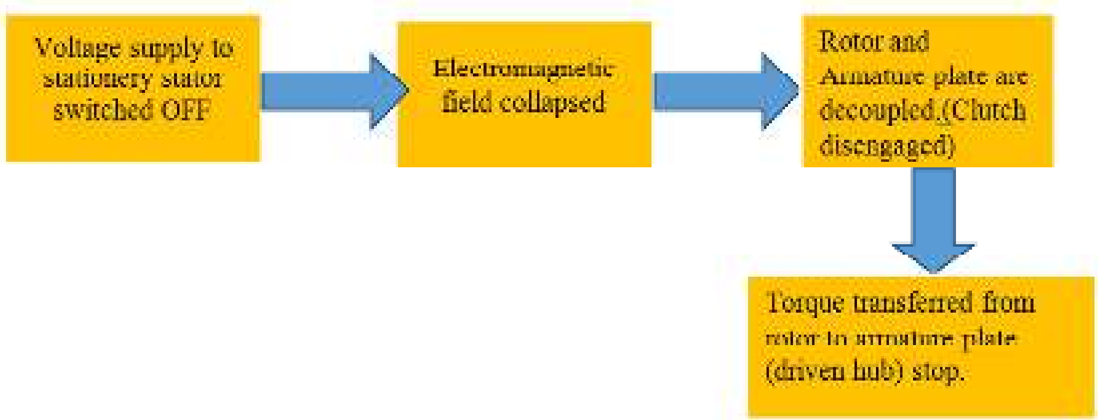

Figure 3.6: Flow charts of EMC disengagement.

3.5. Modeling of the proposed Electromagnetic Clutch system

Once the concept of the EMC system is configured, the mathematical modeling will be carried out. The derivation of the mathematical model for the EMC system is achieved using equivalent model of complete system representation. The electromagnetic constraints of the

EMC system such as electromagnetic force, electromagnetic field density, air gap length, magnetizing force and main dimensions of integrated EMC system will be defined. Finally, the designs of the complete system will be performed to predict behavior of the EMC system.

3.5.1 Equivalent model of the proposed Electromagnetic Clutch system

As shown in figure 3.7, the sectional view of the proposed electromagnetic clutch system explains the basic working principle. The electromagnetic clutch system requires Rotor, armature plate and stationery stator carrying winding sandwiched between them. When voltage supply to stator is ON, electromagnetic flux passes through the first air gap, encircle the stator windings and passes the second air gap again, thereby providing strong electromagnetic force of coupling between the rotor and armature plate. The electromagnetic clutch consists of two air gap (g), the first one is air gap between rotor and stator, the second one is air gap between stator and armature plate. The rotor and armature plate contains slots in which permanent magnets are inserted. The permanent magnet mounted on the surface of rotor and armature plate permits to concentrate the magnetic flux in the air gap (Samuel 2006). Figure 3.7 illustrates Equivalent model of the proposed electromagnetic clutch system.

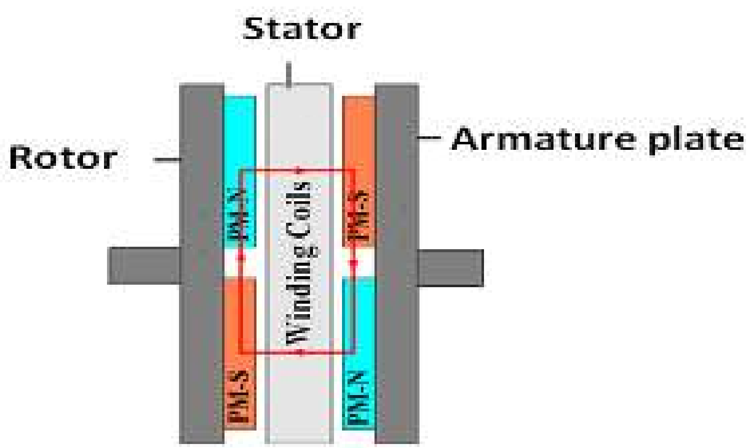

Figure 3.7: Equivalent model of the proposed electromagnetic clutch system.

The magnitude of the electromagnetic force required to couple rotor and armature plate can be calculated as follows (Tomasz , 2009).

$$F_m = \frac{B^2 s}{8\pi} \times 10^7 \text{ ....} (3.1)$$

Where,

F_m	Electromagnetic force [KN]
B	Electromagnetic field [Tesla]
μ_o	Vacuum magnetic permeability and its value is 4π x 10^{-7} Web/Am
S	Effective area of the EMC system [m^2]

The magnitude of the electromagnetic field density required in the air gap length can be defined as follows (Mahmoudi, 2013).

$$B = \frac{NI}{K \times g} \times \mu o \text{ ....} (3.2)$$

Where,

N	Number of turns of the coil
I	Current [A]
K	Ratio of inner diameter to outer diameter
g	Air gap length [mm]

The effective area of the electromagnetic clutch can be defined as follows (Tomasz, 2009).

$$S = \frac{\pi}{4} \times OD^2 \times (1 - K^2) \text{ ....} (3.3)$$

Where, OD is outer diameter and the ratio of outer diameter to inner diameter (K) of the EMC system can be defined as follows (Tamaz, 2009).

$$K = \frac{ID}{OD} \text{ ....} (3.4)$$

Where, ID is inner diameter and axial length of the air gap required for the electromagnetic field density can be defined as follows (Rico, 2012).

$$g = 0.006 \times OD \text{ ....} (3.5)$$

Resistance of the electromagnetic coil can be defined as follows (B.L.Theraja, 2005)

$$R = \frac{\rho \times L}{A_c} \quad (3.6)$$

Where,

R	Resistance of the coil [Ohm]
ρ	Resistivity of copper wire and its value is [Kg/m^3]
A_c	Cross sectional area of the coil [mm^2]
L	Total length of the coil [mm]

Maxwell's Stress Tensor gives a force per unit area produced by the magnetic field applied on effective area of the rotor is defined as follows (Zhang , 2018).

$$q = \frac{B^2}{2\mu o} \quad (3.7)$$

Torque transmitted by the rotor is a function of geometry and magnitude of normal force applied. The normal force is assumed to be uniformly distributed over the effective area of the rotor and attempts to pull the rotor apart. Its effect is similar to those caused by an internally pressurized cylinder and what cause failure in the rotor is typically the tangential stress. The maximum stress that the rotor must handle is tensile strength. By considering uniform pressure theory intensity of the tangential stress can be defined by using the following equation (Gupta, 2005).

$$\sigma_t = \frac{F_n}{A} \quad (3.8)$$

Where,

σ_t	Tangential stress [N/m^2]
F_n	Normal force [N]
A	Effective area of the rotor [m^2]

Since the maximum stress should not exceed the failure strength of the material, safety factor must be developed as follows (Kevin Ludlum, 2013).

$$S_f = \frac{\sigma_f}{\sigma_t} \quad (3.9)$$

Where,

σ_f	Failure strength/Yield strength [N/m^2]
S_f	Safety factor
σ_t	Working/design stress [N/m^2]

Electromagnetic field strength (H_p) required in the air gap length can be defined as follows (B.L.Theraja, 2005).

$$H_p = \frac{B}{\mu_o} \quad (3.10)$$

3.6. Design optimization of the Electromagnetic circuit constraints

3.6.1. Introduction

The design and optimization of the proposed Electromagnetic clutch system (EMCS) is presented in this topic. As mentioned earlier in point 3.4.1, the EMC system is a combination of three parts; rotor, stationery stator and armature plate. Design of the proposed Electromagnetic clutch system should meet performance specification of Toyota 3L, manual transmission listed in table 3.2. Therefore, the next topic presents preliminary design of the proposed EMC system to meet the performance specification of the conventional clutch.

3.6.2. Preliminary design of the proposed Electromagnetic Clutch system

The first design criterion of the proposed EMC system is based on normal force requirement, dimension and space provided for the conventional clutch system. In sizing the components of the EMCS system, the first aspect to be considered is the existence of actual limitations of space. In this regard, like the conventional clutch, there is the possibility to house the proposed EMC system inside the bell house; a limit for the external diameter of the EMC system must be established depending on the diameter of the pressure plate and axial length of bell house; A maximum value of the outer radius of the EMC system is generally considered 275 mm and axial length of bell house is 200mm.Another design requirement is the attainment of an output electromagnetic field strength that is high enough to couple rotor and armature plate. The following section provides the design calculations of the normal force required to hold the clutch in engaged position, effective cross sectional area of the clutch and electromagnetic circuit parameter for the proposed EMC system. According to the operation principle of the friction clutch which belongs to friction disc shown in figure 3.8, Friction disc is held between the flywheel and the pressure plate. Diaphragm spring provides normal force (F_n) to keep the clutch in engaged position (Jiang Kejun, 2015).

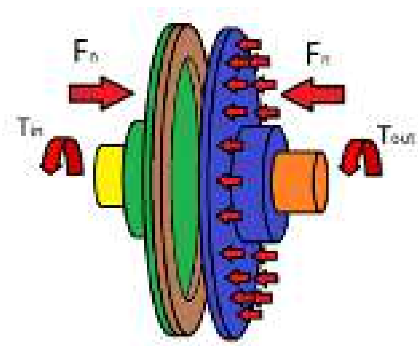

Figure 3.8: Friction disc style clutches (Jessy cussack, 2013).

Considering uniform pressure theory torque transmitted by single plate clutch due to friction can be calculated as: (Jiang Kejun, 2015).

$$T = \mu \times F_n \times R \qquad (3.11)$$

Where,

T	Torque [Nm]
R	Effective radius of friction surface [mm]
F_n	Pressing force [N]
μ	Co efficient of friction

But, effective radius of the friction surface (R) can be defined as follows (Eguchi and T. Yamamoto, 2005).

$$R = \frac{2({R_0}^3 - {R_i}^3)}{3({R_0}^2 - {R_i}^2)} \qquad (3.12)$$

Where,

R_o	Outer radius [mm]
R_i	Inner radius [mm]

From equation 3.12, effective radius of the clutch is calculated as follows:

$$R = \frac{2({R_0}^3 - {R_i}^3)}{3({R_0}^2 - {R_i}^2)}$$

$$R = \frac{2(137.5^3 - 87.5^3)}{3(137.5^2 - 87.5^2)}$$

R=114.35 mm

Therefore, by using equation 3.11, normal force (F_n) required to keep the clutch in engaged position is calculated as:

$$T = \mu \times F_n \times R$$

$$180\text{Nm} = \frac{2}{3} \times 0.2 \times \text{Fn} \times 0.1144\text{m}$$

$$F_n = 7.2 \text{ KN}$$

Assume that the flux density is uniformly distributed over the cross-sectional area. The effective cross sectional area of the EMC system is shown shaded in figure 3.9 below.

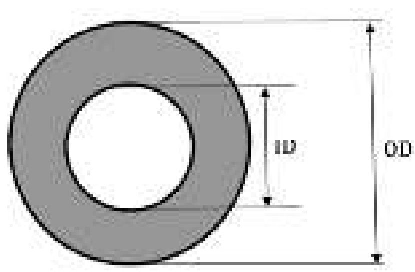

Figure 3.9: Simple geometry of effective area of the EMC system

From equation 3.3, Effective cross sectional area of the EMCS is calculated as:

$$S = \frac{\pi}{4} \times (0.275\text{m})^2 \times (1 - 0.636^2)$$

$$S = 0.036 \text{ m}^2$$

But, effective surface area for double sided excitation should be 2S (Neil Lovell Brown, 2002).Therefore, effective surface area for double sided excitation will be:

$$S = 0.0712 \text{ m}^2$$

The electromagnetic circuit shown in figure 3.7 consists of lines of force, or flux lines that radiate from the stator encircle the two air gaps and pass through the rotor and armature plate. The group of force lines going from the stator is called the electromagnetic flux. The number of lines of force in a electromagnetic field determines the value of the flux. The more lines of force, the greater the flux and the stronger the electromagnetic field. The electromagnetic flux density is the amount of flux per unit area perpendicular to the electromagnetic field. From equation 3.2 maximum normal force of diaphragm spring required to press the clutch in engaged position is calculated as ,7.2KN.Therefore, the magnitude of electromagnetic field required to generate coupling force of 7.2 KN can be calculated from equation 3.1,as follows:

$$F_m = \frac{B^2 s}{8\pi} \times 10^7$$

$$7.2\text{KN} = \frac{B^2 s}{8\pi} \times 10^7$$

$$7.2\text{KN} = \frac{B^2 \times (0.0712)}{8\pi} \times 10^7$$

$$B = \sqrt{\frac{180864}{432000}}$$

$$B = \sqrt{0.4186}$$

$$B = 0.65 \text{ T}$$

Therefore, magnitude of the electromagnetic field required to couple rotor and armature plate is; 0.64 T.As shown in figure 3.10, the electromagnetic clutch consists of two air gap (g), the first one is the air gap between rotor and stator, the second one is air gap between stator and armature plate.

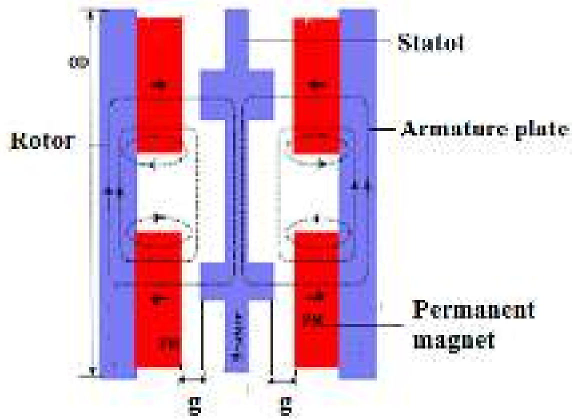

Figure 3.10: Air gap between EMC systems (Tomasz, 2009)

Smaller air gaps produce higher magnetic flux in the air gap but allow less space for windings, (Neil Lovell Brown, 2002).Therefore, The main objective of this calculation part is to determine the optimum value of the air gap length for the proposed EMC system. From equation 3.5, the air gap between the EMC systems is calculated as follows:

$$g = 0.006 \times OD$$

$$g = 0.006 \times OD = 0.006 \times 0.275m$$

$$g = 0.00165m$$

The total length for the two air gap will be 2g which gives us:

$$g = 2 \times 0.00165m = 0.0033m$$

From equation 3.10, strength of the electromagnetic field is calculated as:

$$H_p = \frac{B}{2\mu_o}$$

$$H_p = \frac{0.65}{8\pi \times 10^{-7}}$$

$$H_p = 2.6\times10^5 \text{ A/m}$$

From equation 3.7, energy density force per effective area of the rotor (q) is calculated as follows.

$$q = \frac{B^2}{2\mu o}$$

$$q = \frac{(0.65)^2}{8\pi\times10^{-7}}$$

$$q = 168.2 \text{ KN/m}^2$$

From equation 3.8 the maximum intensity of the tangential stress on the surface of the rotor is calculated as follows.

$$\sigma_t = \frac{F_n}{A}$$

$$\sigma_t = \frac{7200\text{N}}{0.036}$$

$$\sigma_t = 200 \text{ Kpa}$$

The calculated tangential stress on the rotor face must not exceed the failure strength of material .Safety factor of 1 will not be able to handle any additional stress other than the theoretical stress from the design. A safety factor of 2 would be able to handle double the design stress (Kevin Ludlum, 2013). Therefore, from equation 3.9 yield strength of the material can be calculated as follows.

$$\sigma_f = \sigma_t\times S_f$$

$$\sigma_f = 200 \text{ Kpa}\times2$$

$$\sigma_f = 400 \text{ Kpa}$$

From equation 3.4, Ratio of the inner radius to the outer radius (K) is calculated as:

$$K = \frac{Di}{Do} = \frac{175}{275} = 0.636$$

From equation 3.2, we can calculate total number of turns of coil required to produce electromagnetic field density of 0.65T as follows:

$$B = \frac{NI}{k \times g} \times \mu o$$

$$B = 0.65T = \frac{NI}{k \times g} \times \mu o$$

$$NI = \frac{0.65T \times 0.0033 \times 0.063}{8\pi \times 10^{-7}}$$

$$NI = 528 \text{ Turns}$$

The analytical calculation results from the design optimization of the electromagnetic constrains showed that, total number of turns required (NI) =528 is required to achieve electromagnetic flux density of 0.65 T. Moreover, components of the electromagnetic field density are given as a function of dimensional parameters. Thus, optimum geometric structures and physical dimensions of the EMC system should be determined. Choice of stator topology and winding type suitable to design the EMC system are the basis for dimensional parameter optimization (Kevin .S, 2017). The following section explains analytic design optimization of physical dimension for the proposed EMC system.

3.7. Design optimizations of physical dimension for the EMC system

The design of the EMC system is divided in to three stages. The first stage is identifying limitation parameters. The second stage is choosing suitable stator topology and stator winding types. The third stage is calculating optimal dimension for EMC system components .The fourth stage is component design and optimization of discrete parameters of the stator such as, size of pole, size of slot, number of slot, number of pole and poles pitch (Kevin .S, 2017).

3.7. 1.Limitation parameters

These parameter that are characteristics and physical dimensions of EMCS, are considered as the basis for designing. Some of these design limitations are:

- ✓ Limitation of air gap length (g) = 0.0033 m

- ✓ Magnitude of electromagnetic field (B) = 0.65 T
- ✓ Total number of turns of the coil = 528 turns
- ✓ Limitation of maximum axial length = 0.2 m
- ✓ Limitation of maximum outer diameter = 0.275 m
- ✓ Limitation of maximum inner diameter = 0.175 m
- ✓ Effective cross sectional area of the clutch = 0.036m^2

3.7.2. Selection of suitable stator topology

Radial and axial stator configurations can be found regarding the stators position with respect to the rotor positions and the winding arrangements giving freedoms to select the most suitable stator structure into the considered application. The following section discusses the comparison of radial and axial stators for the proposed EMC system application (Peifeng, 2016).

- ✓ Radial flux stator requires more magnet material and is somewhat more complicated to design. The disadvantages of radial flux stator are that the radial stator shape offers few topologies. They also have lower power densities than axial flux stator, and the number of poles is limited by stator diameter.
- ✓ The axial flux stator has much smaller axial length compared with radial stators. Therefore, it needs less volume in the bell house, where there is limited axial length for the EMC system.
- ✓ The axial flux stator has a flux that passes axially so it can be positioned centrally between fly wheel and gear box.
- ✓ There are two basic types of axial flux stator i.e. single-sided or double – sided. Single-sided stator has only one electromagnetic sides and double-sided stator has two electromagnetic sides.
- ✓ Double-sided stator has two working surfaces; allowing more torque to be developed. The back-to-back wound winding is brings advantages such as short end winding length, less copper loss, and simple maintenance

- ✓ Double sided-axial flux stator has good energy efficiency. For the sake of a smaller effective air gap, the stator can be slotted on both sides to enhance the power density. Double flux axial stator increases remarkably the amplitude of the air gap flux density due to shorter air gap. This reduces the required amount of permanent magnets, which yields saving in the price (Peifeng, 2016).

Therefore, double flux axial stator has been chosen as an interesting topology for the design of EMC system. Figure3. 11 show geometric structure of the double flux axial stator.

Figure 3.11: Double flux axial stator structure (Peifeng, 2016).

3.7.3. Choice of stator winding

The windings in stator are keys to the operation and efficiency of the EMC system. There are three different winding layouts possible as summarized below (Yuan & Wan, 2017).

i. Double layer windings use one conductor wire passing though two different stator slots and multiple poles of the machine. Double layer windings reduce the harmonics and provide better efficiency values.

ii. Single winding layouts use one conductor wire wound around one tooth of the stator and only one pole of the machine. They have higher noise and vibrations than double windings.

iii. Toroidal winding layout is wound in a toroidal fashion and has two working surfaces; allowing more torque to be developed. The back-to-back toroidally wound winding is brings advantages such as short end winding length, less copper loss, and simple maintenance .Toroidal windings are used to maximize the use of available space, since they were like triodes around the stator, the axial length of the end windings can be made very short. Therefore, Toroidal windings were chosen as a way to reduce the axial length of the EMC system. Figure3. 12 shows lay outs of the toroidal winding.

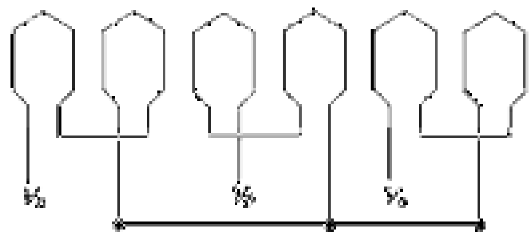

Figure 3.12: Double layer winding layout (Peifeng, 2016)

Double layer toroidal winding features are as follows (Kaliyev, 2015).

- ✓ Double layer toroidal winding means the stator has to halves on the sides of the rotor and side of armature plate, balancing the normal forces acting during EMC operation.
- ✓ Number of coil per stator side = $360^0/ 60^0$ = 6 coils .In total there are 12 stator coils in two side of the stator with winding fill factor (K_{fill}=0.25) and current density of 2.5 A/mm^2.
- ✓ 4 number of group of coils are connected in series to give 2 pole pairs (2P=4pole) and frequency of 50 Hz.
- ✓ 12 stator coils, in total there are: 4 coils per phase, 2 coils per phase per side
- ✓ 3 number of stator winding phase system and number of stator slot per single coil is (q= 2). 4coils are connected in series to give one phase.

3.7.4. The proposed EMC system topology

The double flux stator is located between the two opposing rotor and armature plates. The permanent magnet is mounted on the surface of the rotor and armature plate. Advantage is that the surface-mounted permanent magnets naturally act as fans which have a ventilation effect on the stator and used to concentrate and balance the electromagnetic flux in the air gap. The stator diameter can be change according to its application. In this project, the stator diameter is same as rotor and armature plate diameter.

3.7.5. Sizing equations for axial dimensions of the EMC system

In order to find the optimal dimension of the proposed EMC system, an extensive design space was explored. Having the dimensions of bell house and maximum diameter of the conventional clutch system at hand, axial dimensions of the proposed EMC system can be made. Simplified geometry of the EMC system as shown in figure 3.13, the sizing equations listed below are the basis for the design of EMC system components.

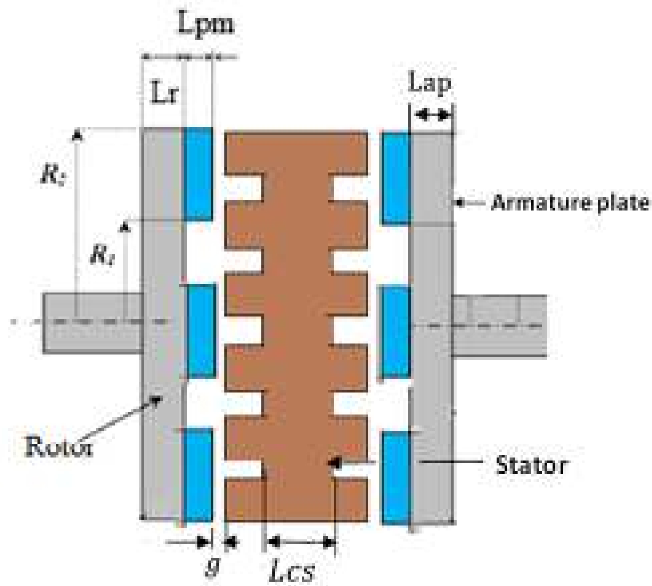

Figure 3.13: Simple geometry of EMC system

Total length of the electromagnetic clutch system can be defined as follows (S.Asghar & Gholamian, 2001).

$$L_e = L_s + L_r + L_{ap} + 2g \qquad (3.13)$$

Where,

L_e Axial length of the EMC system [mm]

L_s	Axial length of the stator [mm]
L_r	Axial length of the rotor [mm]
L_{ap}	Axial length of the armature plate [mm]
g	Axial length of the air gap [mm]

But, axial length of the stator can be defined as follows (Tomasz, 2009).

$$L_s = L_{cs} + 2L_{ss} \quad (3.14)$$

Where,

L_{ss}	Axial length of the stator slot [mm]
L_{sc}	Axial length of the stator core [mm]

A reasonable assumption for calculating the stator slot length, is to assume twice the flux density can be carried in the stator. Axial length of the stator slot can be defined as follows (Tomasz, 2009).

$$L_{ss} = 1.6 \times \frac{\sqrt{Do^2 + \frac{4A_s \times D_g}{K_{fill} \times J_g}}}{2} - D_o \quad (3.15)$$

Where,

D_o	Outer diameter of the stator [mm]
A_s	Cross sectional area of the stator slot [mm^2]
D_g	Average diameter of the stator [mm]
j_g	Current density in winding [A/mm^2]

K_{fill} Winding fill factor

But, cross sectional area of the stator slot can be defined as follows (Nassir, 2009).

$$A_s = \frac{Di}{P} \times L_{stack} \text{.......} (3.16)$$

Where,

D_i Inner diameter of the stator [mm]

L_{stack} Radial length of the stator slot [mm]

P Number of pole

Axial length of the stator core can be defined as follows (Tomasz, 2009).

$$L_{cs} = \frac{B_g \times \pi \times \alpha_p \times Di(1+K)}{4 \times B_{cs} \times p} \text{.......} (3.17)$$

Where,

B_g Electromagnetic field density in the air gap [T]

α_p Pole arc co efficient

B_{sc} Electromagnetic field in the stator core [T]

Axial length of the rotor can be defined as follows (Rhythm, 2016).

$$L_r = L_{cr} + L_{pm} \text{.......} (3.18)$$

Where,

L_{cr} Axial length of the rotor core [mm]

L_{pm} Axial length of permanent magnet [mm]

But, axial length of the rotor core can be defined as follows (Kaliyev, 2015).

$$L_{cr} = \frac{L_{cs}}{2} \text{.......} (3.19)$$

Axial length of the armature plate can be defined as follows (Kaliyev, 2015).

$$L_{ap} = L_{c,ap} + L_{pm} \quad \ldots\ldots\ldots\ldots (3.20)$$

Where, $L_{c,ap}$ is axial length of the armature plate core. Axial length of the permanent magnet can be defined as follows (Neil Lovell & Brown 2002).

$$L_{pm} = \frac{4}{3} \times g \quad \ldots\ldots\ldots\ldots (3.21)$$

Electromagnetic flux density in the stator slot can be defined as follows (Zhang, 2018)

$$B_{cs} = \frac{B_g}{2} \quad \ldots\ldots\ldots\ldots (3.22)$$

Pole arc co efficient can be defined as follows (Werner Eduardo, 2016).

$$\alpha_p = \frac{B_{av}}{B_{max}} \ldots\ldots\ldots\ldots (3.23)$$

Maximum attainable electromagnetic flux density can be defined as follows (S.Asghar & Gholamian, 2001).

$$B_{max} = \frac{2 * \sqrt{3} * B_g}{\pi} \ldots\ldots\ldots\ldots (3.24)$$

Average electromagnetic flux density can be defined as follows (S.Asghar & Gholamian, 2001).

.

$$B_{av} = \frac{2 \times B_{max}}{\pi} \ldots\ldots\ldots\ldots (3.25)$$

Average diameter of the stator can be defined as follows (Ravibala, Singh et al .2016).

$$D_g = \frac{Di + Do}{2} \ldots\ldots\ldots\ldots (3.26)$$

3.7.6 .Calculation for axial dimensions of the EMC system

The EMC system concept covers of various dimensioning equations and towards an initial design; the first natural step to be taken is calculation for axial dimension of the basic structure. Since the outside diameter of the flywheel is fixed and due to the space limitation in the bell house, the outside diameter of the EMC system cannot be larger than 280 mm taking the dimensions into account. Axial length of bell house is fixed. Therefore maximum axial length of the EMC system should not exceed 200mm.Total length of the EMC system is set accordingly to the maximum axial length limitation of bell house. The following section provides calculations of axial dimension for the EMC system components.

From equation 3.15 axial length of the stator slot is calculated as follows:

$$L_{ss} = 1.6\times \frac{\sqrt{Do^2 + \frac{4A_s \times D_g}{K_{fill} \times J_g}}}{2} - D_o$$

But from equation 3.16, area of the stator slot is calculated as follows:

$$A_s = \frac{Di}{P} \times l_{stacl}$$

$$A_s = \frac{0.175}{4} \times (0.275 - 0.175)$$

$$A_s = 0.0437 \text{ m}^2$$

From equation 3.26, Average diameter of the EMC system is calculated as follows:

$$D_g = \frac{Di + Do}{2}$$

$$D_g = \frac{275+175}{2}$$

$$D_g = 225\text{mm} = 0.225\text{m}$$

Therefore, axial length of the stator slot will be:

$$L_{ss} = 1.6\times \frac{\sqrt{(0.275)^2 + \frac{4 \text{ x } 0.00437 \text{ x } 0.225}{0.25 \text{ x } 2.5}}}{2} - 0.275$$

$$L_{ss} = 0.0227 \text{ m}$$

Total axial length slot for double sided stator will be $2\times$ L_{ss} = 0.0454m and from equation 3.17 axial length of the stator slot is calculated as follows:

$$L_{cs} = \frac{B_g \times \pi \times \alpha_p \times D_i(1+K)}{B_{cs} \times 2p}$$

But from equation 3.23, Pole arc coefficient is calculated as follows.

$$\alpha_p = \frac{B_{av}}{B_{max}}$$

From equation 3.24 maximum air gap flux density is calculated as follows:

$$B_{max} = \frac{2 \times \sqrt{3} \times B_g}{\pi}$$

$$B_{max} = \frac{2 \times \sqrt{3} \times 0.65}{\pi} = 0.72 \text{ T}$$

Average air gap flux density can be calculated from equation 3.25 as follows:

$$B_{av} = \frac{2 \times B_{max}}{\pi}$$

$$B_{av} = \frac{2 \times 0.72}{\pi} = 0.45 \text{ T}$$

Therefore, the value of the Pole arc coefficient is calculated as:

$$\alpha_p = \frac{0.45}{0.72} = 0.63$$

From equation 3.22, flux density in the stator core can be calculated as follows:

$$B_{cs} = \frac{B}{2}$$

$$B_{cs} = \frac{0.65}{2} = 0.325\text{T}$$

Therefore, the value of axial length of the stator slot will be;

$$L_{cs} = \frac{0.65 \times \pi \times 0.63 \times 0.175(1+0.636)}{0.325 \times 4p}$$

$$L_{cs} = \frac{0.65 \times \pi \times 0.63 \times 0.175(1 + 0.636)}{0.325 \times 4 \times 4} = 0.0566 \text{ m}$$

From equation 3.21 axial length of the PM is calculated as follows.

$$L_{pm} = \frac{4}{3} \times g$$

$$L_{pm} = \frac{4}{3} \times 0.0033$$

$$L_{pm} = 0.0044 \text{ m}$$

Total axial length of the permanent magnet on rotor and armature plate will be 0.0088m and from equation 3.14 axial length of stator is calculated as follows:

$$L_s = L_{cs} + 2L_{ss}$$

$$L_s = 0.0566 + 0.0454$$

$$L_s = 0.102 \text{ m}$$

From equation 3.18, axial length of rotor is calculated as follows:

$$L_r = L_{cr} + L_{pm}$$

But, from equation 3.19 axial length of rotor core can be calculated as follows:

$$L_{cr} = \frac{L_{cs}}{2}$$

$$L_{cr} = \frac{0.566}{2} = 0.0283 \text{ m}$$

Therefore, axial length of the rotor will be:

$$L_r = 0.0283 + 0.0044 = 0.0322\text{m}$$

From equation 3.20 axial length of armature plate can be calculated as follows:

$$L_{ap} = L_{c,ap} + L_{pm}$$

But axial length of armature plate core can be calculated from equation 3.19 as follows:

$$\mathrm{L}_{c,ap} = \frac{\mathrm{L}_{cs}}{2}$$

$$\mathrm{L}_{c,ap} = \frac{0.566}{2} = 0.0283 \text{ m}$$

Therefore, the value of axial length of armature plate will be:

$$\mathrm{L}_{ap} = 0.0283 + 0.0044 = 0.0322 \text{ m}$$

From equation 3.13, total axial length of the electromagnetic clutch is calculated as follows:

$$\mathrm{L}_{e} = \mathrm{L}_{s} + \mathrm{L}_{r} + \mathrm{L}_{ap} + 2\mathrm{g}$$

$$\mathrm{L}_{e} = 0.102 + 0.0322 + 0.0322 + 0.0033 = 0.1697\text{m} = 169.7 \text{ mm}$$

The analytical calculation result showed that, the outer and inner diameter of the EMC system has been same with that of the conventional friction clutch system. But, total axial length of the EMC system has been 169.7 mm, which is less than axial length of the conventional friction clutch assembly. Therefore, it can be concluded that the EMC system assembly can fit bell house of Toyota 3L, manual transmission.

3.8. Component design for the EMC system

Mechanical design of the components is another important issue in the design analysis of the EMCS. Generally two aspects should be defined for the mechanical design analysis of the electromagnetic clutch system. The first aspect is mechanical structure and materials of the EMC components and the second aspect is field of stress and material strength of the components (Mahmoudi, Kahourzade et al 2013). The following section presents component design for the proposed electromagnetic clutch system.

3.8.1 Design of the permanent magnet

A permanent magnet is an object that is produced from a material that has been magnetized, and produces its own magnetic field. Permanent magnets can be made from materials that are strongly attracted to a magnet, these materials are called ferromagnetic. AlNiCo (Aluminum-Nickel-Cobalt), ferrite (mainly iron), SmCo (Samarium-Cobalt) and NdFeB

(Neodymium-Iron-Boron) are currently the most important types of permanent magnets. Permanent magnets are characterized by their relative permeability (μ_r) which is a measure of ability to conduct magnetic flux, residual induction (B_r) and coercive force (H_c).The comparison of the main PM material is given in table 3.3(Baiba ,2015).

Table 3.2: Comparison of Permanent magnet materials

No	PM materials	μ_r (B/H)	B_r (T)	H_c (KA/m)	B H_{max} (KJ/ m^3)
1	Sr.Ferrite	1.344	0.38	225	27.9
2	Ba.Ferrite	1.114	0.245	175	8.4
3	Smco	1.094	1.1	800	220-240
4	NdFeB	1.061	1.2	900	280-300

The choice of permanent magnets are mainly depends on their operated energy product, which is the product of the field density and the magnetic field strength (BH).Therefore, maximum attainable energy product of the PM required to concentrate electromagnetic field density of 0.65T at an air gap length of 0.0033m is calculated as follows (Baiba , 2015).

$$B\,H_{max} = 0.65\ T \times 258964.96$$

$$B\,H_{max} = 168192.68\ J/m^3 = 168.2\ KJ/m^3$$

From table 3.3.SmCo material has the maximum value of attainable energy product compared with other PM materials. Therefore, SmCo material is chosen as permanent magnet material for the design of EMCS. The shape of the permanent magnet is arc type and its geometrical shape is shown on Figure. 3.14.

Figure 3.14: SmCo material Permanent Magnet shape (Baiba.2015)

The optimum number of PM required on each surface of rotor and armature plate is calculated as follows (Baiba, 2015).

$$N = q\,(2m-1) \qquad (3.27)$$

Where,

N	The optimum number of PM required
m	Number of phase of stator winding
q	Number of stator slot per one stator winding

As mentioned in section 3.7.3 the number of phase of stator winding is 3 and the number of stator slot per one winding is 2. Therefore, from equation 3.27 the number of permanent magnet required for each rotor and armature plate can be calculated as follows.

$$N = q\,(2m-1)$$

$$N = 2\,(2 \times 3-1)$$

$$N = 10$$

The result show that, 10 number of NdFeB permanent magnet are required on each surface of rotor and armature plate to concentrate the electromagnetic field density of 0.65T at an air gap length of 0.0033m.

3.8.2 Design of rotor

The cylindrical body of the rotor contains slots in which the permanent magnets are inserted to concentrate the magnetic flux in the air gap. The rotor has outer diameter and inner diameter of 275mm and 175 mm respectively .The axial length of the rotor is 32.2 mm. The main geometric dimensions of the rotor face with the PM are shown in figure 3.15.

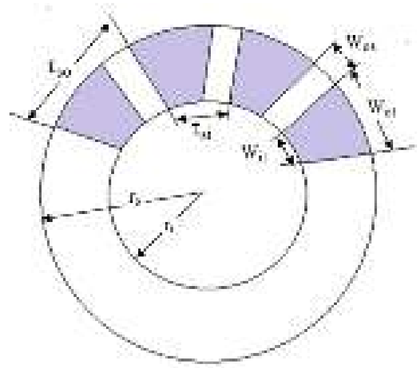

Figure 3.15: Main dimensions of rotor

The first step in the rotor design is to define the dimensions of the rotor. As the outside diameter, inside diameter and axial length has already been determined, only the main dimensions of the PM on the surface of the rotor must to be specified. The sizing equation for geometric dimension of the PM on the surface of the rotor is summarized as follows. Taking the outer radius (r_o) of the rotor as reference, the outer circumference of the rotor can be defined as follows (Kaliyev, 2015).

$$C_o = 2\pi \times r_o \text{ .... (3.28)}$$

Taking the inner radius (r_i) of the rotor as reference, the outer circumference of the rotor can be defined as follows (Kaliyev, 2015).

$$C_i = 2\pi \times r_i \text{ .... (3.29)}$$

Inner pole pitch of the PM on the surface of the rotor can be defined as follows (Jiang, 2015).

$$\tau_{si} = \frac{C_i}{N_{pms}} = W_{it} + W_{os} \text{ .... (3.30)}$$

Where,

τ_{si}	Inner pole pitch [mm]
W_{it}	Permanent magnet bottom width [mm]
W_{os}	Slot width [mm]
N_{pms}	Number of Permanent magnet and slot pairs

Outer pole pitch of the rotor can be defined as follows (Jiang, 2015).

$$\tau_{so} = \frac{C_o}{N_{pms}} = W_{ot} + W_{os} \text{ .... (3.31)}$$

Where,

τ_{so}	outer pole pitch [mm]
W_{ot}	Permanent magnet top width [mm]
W_{os}	Slot width [mm]
N_{pms}	Number of Permanent magnet and slot pairs

Slot width of the rotor can be defined as follows.

$$W_{os} = \frac{\tau_p \times B}{B_{max}} \text{.. (3.32)}$$

Average pole pitch (τ_p) of the rotor can be defined as follows (Jiang, 2015).

$$\tau_p = \frac{\pi \times D_{ave}}{2 \times N_{pms}} \text{... (3.33)}$$

From equation 3.28 and 3.29, outer circumference and inner circumference of the rotor respectively can be calculated as follows:

$$\text{Co} = 2\pi \times 0.1375 = 0.864 \text{ m}$$

$$\text{Ci} = 2\pi \times 0.0875 = 0.549 \text{ m}$$

$$\tau_p = \frac{\pi \times 0.225}{2 \times 10} = 0.0241\text{m}$$

From equation 3.32, width of the slot can be calculated as:

$$W_{os} = \frac{\tau_p \times B}{B_{max}}$$

$$W_{os} = \frac{0.0241 \times 0.65}{0.72} = 0.0266 \text{ m}$$

From equation 3.30, top width of the permanent magnet can be calculated as:

$$\tau_{si} = \frac{C_i}{N_{pms}} = \frac{0.549}{10} = 0.0549 = W_{it} + W_{os}$$

$$W_{it} = 0.0549 - W_{os}$$

$$W_{it} = 0.0549 - 0.0266$$

$$W_{it} = 0.0283 \text{ m}$$

From equation 3.31, bottom width of the permanent magnet can be calculated as:

$$\tau_{so} = \frac{C_o}{N_{pms}} = \frac{0.864}{10} = 0.0864 = W_{ot} + W_{os}$$

$$W_{ot} = 0.0864 - W_{os}$$

$$W_{ot} = 0.0864 - 0.0266$$

$$W_{ot} = 0.0562 \text{ m}$$

Table 3.3: Design dimensions of the rotor

No	Parameters	Values	SI unit
1	The number of slot (N_s)	10	-
2	The number of pm	10	-
3	Axial length of the rotor	32.2	mm
4	Permanent magnet top width	56.2	mm
5	Permanent magnet bottom width	28.3	mm
6	Width of the slot	26.6	mm

i. Material selection for rotor

Operating the rotor at a normal force of 7200N and a rotational speed of 4800 rpm produces the rotor material selection choices in two ways. The tangential stresses and rotational stress on the rotor demand high strength material. In addition to the strength, electrical properties that the material should posses contribute to the choice of material. The following are desirable mechanical and electrical properties of material for the rotor.

a) Desirable mechanical properties of the material.

Some of the mechanical properties that a material for the rotor should possess are listed below.

- The material must handle yield strength of 400 Kpa.
- The material must handle centrifugal stress due to rotation of the rotor which is defined as follows (P.Kattimani, 2018).

$$\sigma_t = \rho \times \omega^2 \times R^2 \qquad (3.34)$$

Where,

ω	Angular velocity [rad/sec]
ρ	Density of the material [Kg/m^3]
R	Outer radius of the rotor[m]

Angular velocity and radius of the rotor are constant. Usually the key for material that can handle the stress due to rotation is material with the highest possible density.

b) Desirable electrical properties of the material.

Some of the electrical properties that a material for the rotor should possess are listed below.

- ✓ Minimum electromagnetic flux density (B) of 0.65 T.
- ✓ Minimum energy density force per area (q) of $168.2 KN/m^2$.
- ✓ Minimum Coercive force (H_c). Coercivity expresses the ability of the material to retain its magnetized state. Minimum Coercive force means minimum resistance of the material to the applied electromagnetic field. This force permits rapid demagnetization of the material (Kaliyev 2015).
- ✓ Good magnetic conductivity (σ) (Drapala, 2014).

✓ Maximum energy product - By definition, magnetic energy is the product of the induction in the magnet (electromagnetic fled strength) and the magnetizing force it took to excite the material. Attainable magnetizing energy (E) of the rotor can be calculated as follows (Drapala, 2014).

$$E = B\,H_{max} \qquad (3.35)$$

$$B\,H_{max} = 0.65\text{ T x } 258964.96$$

$$B\,H_{max} = 168192.68\text{ J/m}^3 = 168.2\text{ KJ/m}^3$$

Commonly, the following materials are employed as materials for the design of high speed rotor.

i. **Silicon-iron Alloys.** The alloys containing between 10 and 40 % Si .They represent the best possible combination between good magnetic and mechanical properties. This material offers highest yield strength ranging 450 to 610 Kpa. Their magnetizing energy ranges 200 to 300.This material provides highest electrical conductivity and operating electromagnetic field range of 0.6 to 0.83T , while providing maximum density of 852 to 875Kg/m^3 (Gavril &V. Ionita , 2002).

ii. **Nickel-iron alloys**. The Fe-Ni alloys, often called perm alloys, are the most versatile from all the known magnetic materials. The alloys containing between 30 and 80 % Ni and 50%Ni have high saturation magnetization and low Ni content have a high electrical resistance. This material offers lowest yield strength ranging 360 to 420Kpa and the maximum magnetizing energy range of 160-180 KJ/m^3 (Gavril &V. Ionita, 2002). They have has operating electromagnetic field range of 1.5 to 2.1T and lowest density range of 785 to 790 Kg/m^3 (Drapala, 2014).

iii. **Soft Ferrites.** These materials are ferromagnetic with a cubic crystal structure and the general composition of manganese or zinc, nickel and iron. These materials can be easily magnetized and great amplification of electromagnetic field produced by electric current in the coil and has operating electromagnetic field of about 1T (Tiberto, 2015). However, while their magnetic performance is attractive, the mechanical properties of these materials are inadequate for high speed application .They offers lowest yield strength ranging 220 to 310Kpa and the highest permeability ranges 100 to 300.Their density ranges 650 to 745 kg/m^3 (Gavril &V. Ionita , 2002).

Therefore, Silicon-iron alloy, 26% Si-Fe is chosen as the material for the rotor. Property of the material is listed in table 3.5.

Table 3.4: Properties of the 16% Si-Fe material for the design of rotor (Tiberto, 2015)

No	Property	Values	SI unit
1	Operating electromagnetic field density(B)	0.71	T
2	Electric conductivity (σ)	2.5x10^6	J/Kg
3	Coercivity (H_c)	0.02	A/m
4	Yield strength	520	Kpa
5	Energy density force per area (q)	375	KN/m^2
6	Density (ρ)	874	Kg/m^3
7	Energy product (E)	230	KJ/m^3

ii. 3D modeling of rotor

The rotor is cylindrical iron with a thickness of 32.2mm. Outer diameter and inner diameter of the rotor is 275 mm and 175 mm respectively. The stator side of the rotor has a set of 10 equally spaced Smco permanent magnets arranged on its circumference. This permits the electromagnetic flux density to be concentrated in the air gap.Figure3. 16 show 3D modeling of the rotor by using CAD software.

Figure 3.16: 3D view of the rotor

3.8.3 Design of the stator

The stator has double flux cylindrical geometry as discussed in section 3.7.2 and geometric properties of the stator such as, axial length of the stator slot, axial length of the stator core, top and bottom width of the stator teeth, pole pitch, number of slots and number of teeth are the key point to define the stator geometry (Werner Eduardo, 2016).In order to find the optimal dimension of the stator geometry, an extensive design space was explored. In this point we can make some preliminary analytical calculations to estimate the main geometric dimensions of the stator, limited by the axial length of the stator and the stator diameter. Figure 3.17 shows 2D geometric structure of the stator.

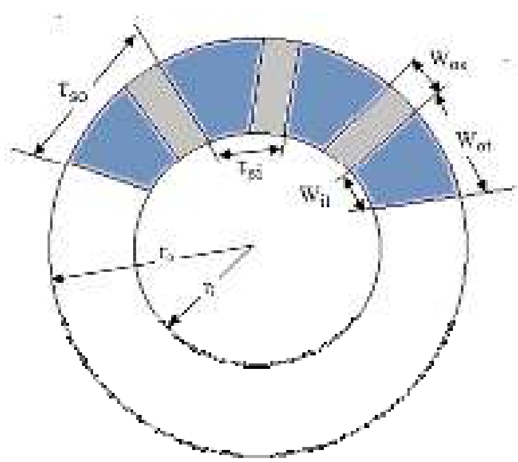

Figure 3.17: Main dimension of the stator (Werner Eduardo, 2016).

Taking the outer and inner diameter of the stator as reference, it is possible to express geometric dimension of the stator. Total number of stator teeth and stator slot can be defined as follows (Werner Eduardo, 2016).

$$Q = m \times 2P \times q \quad (3.36)$$

Where,

Q	Total number of teeth and slot of the stator
m	Number of phase
P	Number of pole
q	Number of stator slot per single coil

Taking the outer radius (r_o) of the stator as reference, the outer circumference of the stator can be defined as follows (Werner Eduardo, 2016).

$$C_o = 2\pi \times r_o \quad (3.37)$$

Taking the inner radius (r_i) of the stator as reference, the inner circumference of the stator can be defined as follows (Werner Eduardo, 2016).

$$C_i = 2\pi \times r_i \quad (3.38)$$

Inner pole pitch of the stator can be defined as follows (Asghar.S & Gholamian , 2001).

$$\tau_{si} = \frac{C_i}{N_{ss}} = W_{it} + W_{os} \quad (3.39)$$

Where,

τ_{si}	Inner pole pitch of the stator [mm]
W_{it}	Bottom width of the stator teeth [mm]
W_{os}	Slot width of the stator [mm]
N_{ss}	Number of stator teeth and slot per one side

Outer pole pitch of the rotor can be defined as follows (Asghar.S & Gholamian, 2001).

$$\tau_{so} = \frac{C_o}{N_{ss}} = W_{ot} + W_{os} \quad (3.40)$$

Where,

τ_{so}	Outer pole pitch of the stator [mm]
W_{ot}	Top width of the stator teeth [mm]

Slot width of the stator can be defined as follows (Sahin, 2001).

$$W_{os} = \frac{\tau_p \times B}{B_{max}} \quad (3.41)$$

Average pole pitch (τ_p) of the stator can be defined as follows (Sahin, 2001).

$$\tau_p = \frac{\pi \times D_{ave}}{2 \times N_{ss}} \quad (3.42)$$

The value of m, 2p, q are mentioned in section 3.7.3, Therefore, from equation3.36. Total number of teeth and slot required for the stator is calculated as follows:

$$Q = m \times 2P \times q$$

$$Q = 3 \times 4 \times 2$$

$$Q = 24$$

The result shows that 12 numbers of teeth and slot is required for one side of the stator. From equation 3.37 and 3.38; outer circumference and inner circumference of the stator can be calculated as follows respectively:

$$C_o = 2\pi \times 0.1375 = 0.864 \text{ m}$$

$$C_i = 2\pi \times 0.0875 = 0.549 \text{ m}$$

From equation 3.42 average pole pitches is calculated as follows.

$$\tau_p = \frac{\pi \times 0.225}{2 \times 12} = 0.0294 \text{ m}$$

From equation 3.41, width of the stator slot can be calculated as:

$$W_{os} = \frac{\tau_p \times B}{B_{max}}$$

$$W_{os} = \frac{0.0294 \times 0.65}{0.72} = 0.0266 \text{ m}$$

From equation 3.39, top width of the stator teeth can be calculated as:

$$\tau_{si} = \frac{C_i}{N_{ss}} = \frac{0.549}{12} = 0.0458 = W_{it} + W_{os}$$

$$W_{it} = 0.0458 - W_{os}$$

$$W_{it} = 0.0458 - 0.0266$$

$$W_{it} = 0.0192 \text{ m}$$

From equation 3.40, bottom width of the stator teeth can be calculated as follows:

$$\tau_{so} = \frac{C_o}{N_{ss}} = \frac{0.864}{12} = 0.0724 = W_{ot} + W_{os}$$

$$W_{ot} = 0.0724 - W_{os}$$

$$W_{ot} = 0.0724 - 0.0266 = 0.0454 \text{ m}$$

Taking the outer diameter and axial length of the stator as the reference, geometric dimension of the stator is shown in table 3.6 as follows:

Table 3.5: Design dimensions of the stator

No	Parameters	Values	SI unit
1	Average diameter of the stator	225	mm
2	Axial length of the stator	102	mm
3	Number of slot	24	-
4	Number of teeth	24	-
5	The number of coil per stator side	6	mm
6	Top width of the stator tooth	45.4	mm
7	Bottom width of the stator tooth	19.2	mm
8	The width of stator slot (Ws)	26.6	mm
9	The number of phase	3	

10	The depth of slot/axial length of stator slot (D_s)	28.2	mm

i. 3D modeling of the stator

The stator does not rotate. Thus, there are typically low stresses and forces during operation. Stators are usually made from steel. The steel used is magnetic, and has good properties for electromagnetic induction (Kevin, 2017). It has outer diameter of 275 mm and inner diameter of 175mm with axial length of 102 mm. In total, the stator has 24 slots for the electrical winding to pass through. The shape and size of the slots was optimized for the EMC application. Figure3. 18 show the 3D view of the stator by using CAD software.

Figure 3.18: 3D view of the stator

3.8.4 Design of stator winding

This section provides selection of optimum winding diameter and design calculation of main parameter of the winding such as cross sectional area, total length of the coil and resistance of the coil. In order to achieve a required magnetic field strength, a coil of *N* turns can be constructed as shown in figure 3.19. The coil is formed by wrapping a conductor around the stator slot. The magnetic field strength is directly proportional to the number of turns of the winding, as well as parameters of the winding (Nassir, 2009).

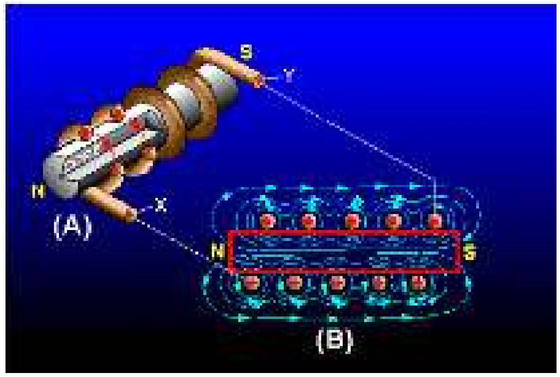

Figure 3.19: Magnetic field produced by current carrying coil (Nassir, 2009)

Total length of the winding (L_{total}) is determined by the following equations (Nassir, 2009).

$$L_{total} = 2N_{turns}\ [L_s + L_{ss} + [\frac{W_{os}}{N_{slot}} \times (D_i\ + h_{slot})\pi \ldots\ldots\ldots\ldots\ldots (3.43)$$

Where,

N_{turns}	Total number of turns of the coil
L_{total}	Total length of copper coil [mm]
L_{ss}	Axial length of the stator slot [mm]
h_{slot}	Height of stator slot [mm]
L_s	Axial length of the stator [mm]
D_i	Inner diameter of the stator [mm]
N_{slot}	Total number of the stator slot
W_{os}	Width of the stator slot [mm]

Cross sectional area (A_c) of the coil can be estimated by the following equations (Erickson, Chen et al. 2001).

$$A_c = \frac{A_{total\,slot} \times k_{fill}}{2N_{turns}} \ldots\ldots\ldots\ldots\ldots\ldots\ldots\ldots\ldots\ldots\ldots\ldots\ldots (3.44)$$

Where,

N_{turns}	Total number of turns of the coil

$A_{total,slot}$	Total cross sectional area of stator slot [mm^2]
K_{fill}	Winding fill factor

Total cross sectional area ($A_{total,slot}$) of the stator can be determined by the following equations (Nassir, 2009).

$$A_{total\ slot} = 24\ [\frac{1}{2} \times h_{slot}(W_{ot} + W_{it}) \ \text{...} \ (3.45)$$

Where,

h_{slot}	Height of stator slot [mm]
W_{it}	Bottom width of the stator teeth [mm]
W_{ot}	Top width of the stator teeth [mm]

Resistance of the coil can be determined as follows (B.L.Theraja, 2005).

$$R = \frac{\rho \times L}{A_c} \text{...} \ (3.46)$$

Where,

R	Resistance of the coil [Ohm]
ρ	Resistivity of copper coil 1.724 x 10^{-6} ahm.cm
A_c	Cross sectional area of coil [mm^2]
L_{total}	Total length of copper coil [mm]

In section 3.5 the total number of turns required (NI) required achieving electromagnetic flux density of 0.65 T is determined as 528 turns. From equation 3.43, total length of the winding can be calculated as follows.

$$L_{total} = 2N_{turns}\ [L_s + L_{ss} + [\frac{W_{os}}{N_{slot}} \times (D_i + h_{slot})\pi$$

$$L_{total} = 2\times528 \ [0.102 + 0.0454 + [\frac{0.0266}{24}\times(0.175 + 0.001)\pi \ ]$$

$$L_{total} = 147 \text{ m}$$

From equation 3.45, total area of the stator slot is calculated as follows.

$$A_{total\ slot} = 24[\frac{1}{2}\times h_{slot}(W_{ot} \ + W_{it} \ )$$

$$A_{total\ slot} = 24[\frac{1}{2}\times 0.001(45.4 + 19.2)$$

$$A_{total\ slot} = 1968 \text{ mm}^2$$

From equation 3.44 cross sectional area of the winding can be estimated as follows.

$$A_c = \frac{A_{total\ slot}\times k_{fill}}{2N_{turns}}$$

$$A_c = \frac{1968\times0.25}{2\times528}$$

$$A_c = 0.91 \text{ mm}^2$$

By using the value of cross sectional area of the winding the diameter of the winding can be calculated as follows.

$$d_c = \sqrt{\frac{4\times A_c}{4}} = \sqrt{\frac{4\times 0.91}{4}}$$

$$d_c = 1.075 \text{ mm}$$

Now suitable size of the winding can be expressed. The standard method used to express wire size is the American Wire Gauge (AWG) system and the optimum diameter of the wire should be less than or equal to estimated value of the coil diameter (Arthur & Williams, 2011).From American standard of wire gauge diameter, diameter of coil is chosen as: d= 1.024 mm. Therefore, cross sectional area of the coil can be calculated as follows:

$$A_c = \pi r^2 = \pi(0.512)^2 = 0.823\text{mm}^2$$

From equation 3.46 we can calculate resistance of the coil as follows:

$$R = \frac{\rho \times L}{A_c}$$

It is known that resistivity of copper coil is given in terms of ohm.cm. Therefore, to calculate resistance of the coil the units of A_C and L should be substituted in terms of cm.

$$Ac = 0.00823cm^2 \text{ and } L = 14700cm$$

$$R = \frac{1.724 \times 10^{-6} \times 14700}{0.00823}$$

$$R = 3.11\ ohm$$

3.8.5 Design of armature plate

The armature plate has cylindrical core with axial length of 32.2 mm and 10 permanent magnets are embedded in to its cylindrical core for better flux distribution in the air gap between the stator and armature plate. The detail geometric dimension of the armature plate is shown in figure 3.20.

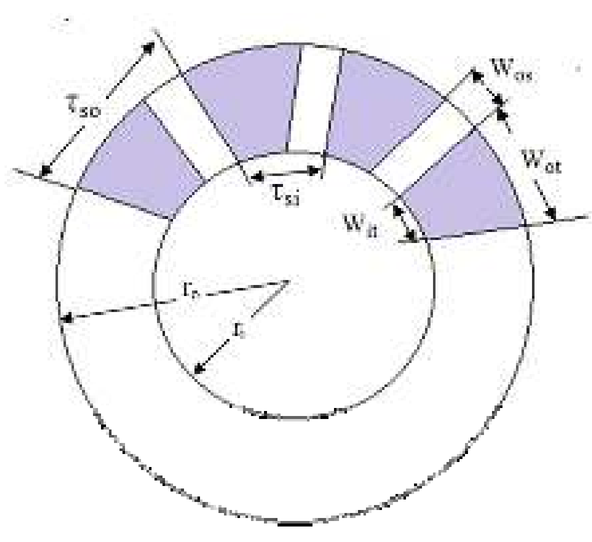

Figure 3.20: Main dimensions of the armature plate

The first step in the armature design is to define the geometric dimension of the armature plate as for the design of the rotor. As the outside diameter, inside diameter and axial length has already been determined, only the main dimensions of the PM on the surface of the armature plate must to be specified. The sizing equation for the armature plate can be summarized as follows: Taking the outer radius (r_o) of the armature plate as reference, the outer circumference of the armature plate can be defined as follows (Kaliyev, 2015).

$$C_o = 2\pi \times r_o \qquad (3.47)$$

Taking the inner radius (r_i) of the armature plate as reference, the outer circumference of the armature plate can be defined as follows (Kaliyev, 2015).

$$C_i = 2\pi \times r_i \qquad (3.48)$$

Inner pole pitch of the armature plate can be defined as follows (Kaliyev, 2015).

$$\tau_{si} = \frac{C_i}{N_{pms}} = W_{it} + W_{os} \qquad (3.49)$$

Where,

τ_{si}	Inner pole pitch [mm]
W_{it}	Permanent magnet bottom width [mm]
W_{os}	Slot width [mm]
N_{pms}	Number of Permanent magnet and slot pairs

Outer pole pitch of the armature plate can be defined as follows (Kaliyev, 2015).

$$\tau_{so} = \frac{C_o}{N_{pms}} = W_{ot} + W_{os} \qquad (3.50)$$

Where,

τ_{so}	Outer pole pitch [mm]
W_{ot}	Permanent magnet top width [mm]
W_{os}	Slot width [mm]
N_{pms}	Number of Permanent magnet and slot pairs

Slot width of the armature plate can be defined as follows (Yuan & Wan, 2017).

$$W_{os} = \frac{\tau_p \times B}{B_{max}} \qquad (3.51)$$

Average pole pitch (τ_p) of the armature plate can be defined as follows (Kaliyev, 2015).

$$\tau_p = \frac{\pi \times D_{ave}}{2 \times N_{pms}} \qquad (3.52)$$

i. Calculation for main dimensions of the armature plate

From equation 3.47 and 3.48, outer circumference and inner circumference of the armature plate can be calculated as follows respectively:

$$C_o = 2\pi \text{ x } 0.1375 = 0.864 \text{ m}$$

$$C_i = 2\pi \text{ x } 0.0875 = 0.549 \text{ m}$$

From equation 3.52, average pole pitch of the PM is calculated as:

$$\tau_p = \frac{\pi \times 0.225}{2 \times 10} = 0.0241 \text{ m}$$

From equation 3.51, width of the slot can be calculated as:

$$W_{os} = \frac{\tau_p \times B}{B_{max}}$$

$$W_{os} = \frac{0.0241 \times 0.65}{0.72} = 0.0266 \text{ m}$$

Now, top width of the PM can be calculated from equation 3.49, as follows:

$$\tau_{si} = \frac{C_i}{N_{pms}} = \frac{0.549}{10} = 0.0549 = W_{it} + W_{os}$$

$$W_{it} = 0.0549 - W_{os}$$

$$W_{it} = 0.0549 - 0.0266$$

$$W_{it} = 0.0283 \text{ m}$$

Bottom width of the PM can be calculated from equation 3.50 as follows:

$$\tau_{so} = \frac{C_o}{N_{pms}} = \frac{0.864}{10} = 0.0864 = W_{ot} + W_{os}$$

$$W_{ot} = 0.0864 - W_{os}$$

$$W_{ot} = 0.0864 - 0.0266$$

$$W_{ot} = 0.0562 \text{ m}$$

Table 3.6: Design dimensions of the armature plate

No	Parameters	Values	SI unit
1	The number of total slot (N_s)	10	-
2	The number of pm	10	-
3	Axial length of the armature plate	32.2	mm
4	Permanent magnet top width	56.2	mm
5	Permanent magnet bottom width	28.3	mm
6	Width of the slot	26.6	mm

ii. Material selection for the armature plate

Torque transmitted by the EMC is a function of geometry and magnitude of normal force applied by the electromagnet. The applied electromagnetic force keeps the EMC in engaged position with uniform pressure all over its contact area. The consequently analysis is based on uniform pressure theory. The structural material of the armature plate should have the following properties (Kevin Ludlum, 2013).

A) Strength- ability to with stand maximum stress due normal force (F_n) applied on contact area of the armature plate (A) which can be calculated as equations.

$$\sigma = \frac{F}{A} \qquad (3.53)$$

Where,

σ_t	Tangential stress [N/m^2]
F_n	Normal force [N]
A	Effective area of the rotor [m]

From

equation 3.53 maximum stresses on the armature plate is calculated as follow.

$$\sigma = \frac{F}{A}$$

$$\sigma = \frac{7200N}{0.036}$$

$$\sigma = 200 \text{ Kpa}$$

Since the maximum stress should not exceed the failure strength of the material, safety factor must be developed. Safety factor of 1 will not be able to handle any additional stress other than the theoretical stress from the design. A safety factor of 2 would be able to handle double the design stress. A safety factor of less than 1 is not at all acceptable in design (Kevin Ludlum, 2013).The calculated tangential stress on the armature plate face must not exceed the failure strength of material. Therefore, material properties such as yield strength have associated tolerance that must be considered. By using maximum strain principal theory Failure strength of the material is calculated as follows (Gupta, 2005).

$$\sigma_f = \sigma_t \times S_f \text{ .... (3.54)}$$

Where,

σ_f	Failure strength/Yield strength [N/m^2]
S_f	Safety factor
σ_t	Working stress [N/m^2]

$\sigma_f = 200$ Kpa $\times 2$

$\sigma_f = 400$ Kpa

From equation 3.35 failure strength/yield strength of the material can be calculated as follows.

$$\sigma_f = 200 \text{ Kpa} \times 2$$

$$\sigma_f = 400 \text{ Kpa}$$

B) Minimum time constant – it is a measure of the expected time required for the rotating armature plate to stop. It can be calculated by using the following equations (Rhythm, 2016).

$$\tau = \frac{I}{b} = \frac{2\rho \times R^2}{n \times \sigma \times D^2 \times B^2} \quad (3.55)$$

$$b = n\frac{\pi \times \sigma}{4} D^2 \times d \times B^2 \times R^2 \quad (3.56)$$

$$I = \frac{1}{2} d \times \pi \times \rho \times R^2 \quad (3.57)$$

Where,

τ	Time constant [s]
b	Effective damping coefficient [Nm s]
I	Moment of inertia of the material [kg m^2]
σ	Specific conductivity of the material [J/Kg]
ρ	Density of the material [Kg/m^3]
R	Maximum radius [m]
D	Stiffness of the material [Nm/Kg]
B	Thickness of plate [mm]
n	Number of plate

The material for the armature plate must be optimized in order to minimize the time constant (τ) and minimize the disc's moment of inertia (I). In order to minimize the time constant, we must choose the smallest ratio of density to conductivity from all the materials available (Rhythm, 2016).There are two strong candidates in my selection of material for the armature plate which are Alloy steel ADTM 1010 and Steel Fe 290. The key for material selection of the armature plate is the highest possible yield strength over minimum time constant. Property of the material is shown in table 3.8 (Gupta, 2005).The required electrical properties of the material for the armature plate will be same with that of material for the rotor.

Table 3.7: Properties of structural steel and Alloy materials (Gupta, et.al, 2005)

Materials	Density [Kg/m^3]	electric conductivity [J/kg]	Yield strength [Mpa]	Flux density (T)	Energy density[KJ/m^3
Alloy steel ADTM 1010	7850	60 x 10^6	180	0.74	242
Steel Fe 290	7200	50 x 10^6	170	0.82	215

Comparison between the two materials is based on the qualitative result of Equation 3.55, 3.56 and 3.57. In order to choose material with minimum time constant, we must compare the smallest ratio of density to conductivity of the two materials. The expected time constant for Alloy steel ADTM1010 material is calculated as follows:

$$\tau = \frac{\rho}{\sigma} = \frac{7850}{60000000}$$

$$\tau = 1.3 \text{ x } 10^{-4} \text{ kg m}^2/\text{S}$$

The expected time constant for Steel Fe 290material is calculated as follows:

$$\tau = \frac{\rho}{\sigma} = \frac{7200}{50000000}$$

$$\tau = 1.44 \text{ X}10^{-4} \text{ kg } m^2/\text{S}$$

iii. 3D modeling of the armature plate

The time constant comparison result shows that, Alloy steel ADTM1010 material has minimum expected time constant. Therefore, Alloy steel ADTM1010 is chosen as the material for armature plate in order to achieve better performance.Figure3. 21 show 3D view of the armature plate by using CAD software.

Figure 3.21: 3D view of the armature plate

The armature plate has outer and inner diameter of 275mm and 175 mm respectively.10 pm of the same dimension are arranged on the surface of the armature plate to concentrate electromagnetic field between the air gaps.

3.8.6 Assembly of the EMC system

The electromagnetic clutch is a media between the powered rotation transfers from rotor to the gear box via the armature plate. The rotor is normally connected to the part that is always moving with the engine (flywheel). The armature plate is connected to the component that requires the acceleration (output shaft). The stator was held stationery and is sandwiched between rotor and armature plate. Figure 3.22 shows 3D assembly view of the EMC system.

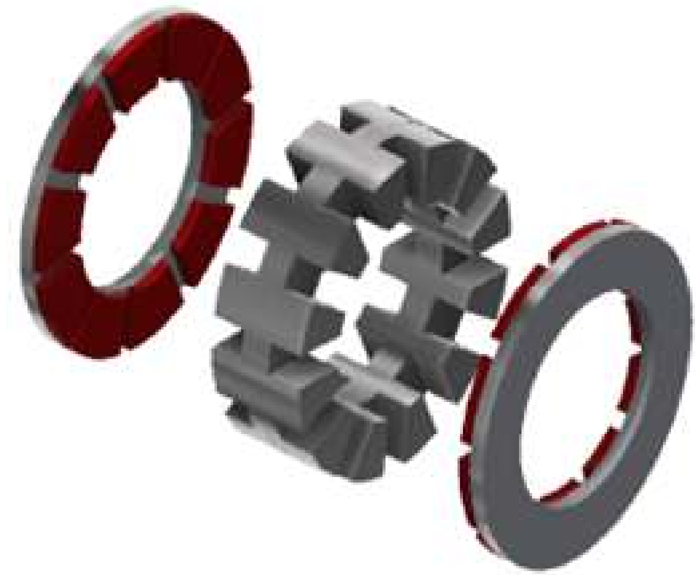

Figure 3.22: Assembly of the EMC system

There are two air gaps between rotor and armature plate. The cylindrical body of the rotor and armature plate contains 20 permanent magnets in total to concentrate electromagnetic flux in the air gap. Dimension of the EMC system was designed according to standard dimensions of Toyota 3L, manual transmission and the EMC system can be directly fitted onto bell housing of the conventional clutch.

CHAPTER FOUR

4. RESULT AND DISCUSSION

In the existing clutch system shown in figure 4.1, flywheel, friction disc, pressure plate and diaphragm spring are used to transmit mechanical torque between engine and gear box of Toyota 3L, manual transmission. The car engine was only capable of delivering a gross mechanical power of 68kW (91hp) and peak torque of 180Nm at 4800rpm. Bell house of the car has maximum axial length of 200mm.Pressure plate has outer diameter of 275 mm and inner diameter of 17mm.

Figure 4.1: Toyota 3L, manual transmission clutch system.

Equation 2.1 shows that torque transmitted by the existing friction clutch system is a function of mechanical force, co efficient of friction and effective radius of the clutch. Toward the goal of maximizing torque, the existing friction clutch system has used high friction composite material to maximize coefficient of friction. Torque capacity of the friction clutch system is then limited to only the amount of mechanical force that can be applied by diaphragm spring. Analytical calculation results from equation 3.11 showed that to transmit engine torque of 180Nm, mechanical force of 7.2KN is applied by the diaphragm spring to engage flywheel and pressure plate of the existing friction clutch system. This mechanical force is not constant; it tends to decreases with the decrease in thickness of the friction disc due to wear. These characteristics are reported to have loose of torque due to friction disc that slip between flywheel and pressure plate (Cappetti &Mario, 2012). The reductions in this mechanical force have also an influence on vehicle comfort. Too light pedal force makes drivers feel the juncture not obviously (Jiangchuan &Feng, 2013). Another problem with this mechanical force is that it is not equally distributed over the contact area of the friction surface and it has influence on contact properties of the friction clutch. The real area of contact is only a small percentage of the nominal surface area. Wear occurs on the uppermost regions of the friction material during sliding. The outer resin layer will probably be lost in the first instance, but the inner cellulose fibers and regions of filler materials may also be lost, as the wear of the material continues. During the operation of a friction material it will wear, which can affect the performance of the clutch (GAO & Barber, 2002).

However, in the proposed EMC system, rotor, double face axial stator and armature plate transmits mechanical torque between engine and gear box of Toyota 3L, manual transmission. The bell house of the car is assumed to enclose the EMC system. The rotor is normally connected to the part that is always moving with the engine. The armature plate is connected to the component that requires the acceleration. The double face axial stator is sandwiched between the rotor and armature plate. The EMC system is activated by applying a direct current to the stator coil. This creates a magnetic field, which electromagnetically couple the rotor with armature plate and so allows torque to be transmitted from engine to gear box. Torque is transmitted magnetically and there are no mechanically contacting parts. This shows that no wear occur to the torque transfer components of the proposed EMC system compared with the existing clutch system. Most aspects of the proposed EMC system design optimization were determined by its electromagnetic circuit parameters and geometric dimension parameters. The electromagnetic circuit design optimization that took place was to fix the electromagnetic circuit constraints in to the required electromagnetic coupling force of 7.2 KN. The geometric dimension design optimization that took place was to fit the EMC system assembly in to the fixed dimension of the existing bell house. The results of the electromagnetic clutch system design are listed in table 4.1.

Table 4.1: Detail design analysis of the EMC system

No	Specification	Value	Unit
1	Total axial length of the EMC assembly	169.7	mm
2	Axial length of stator core	56.6	mm
3	Total axial length of stator slot	45.4	mm
4	Axial length of stator	102	mm
5	Axial length of rotor	32.2	mm
6	Axial length of armature plate	32.2	mm
7	Axial length of permanent magnet	4.4	mm
8	Top width of the permanent magnet	56.2	mm
9	Bottom width of the permanent magnet	28.3	mm
10	Total axial length of air gap	3.3	mm
11	Surface area of armature plate	0.036	m^2

12	Clutch coupling force	7200	N
13	Electromagnetic field density in the air gap (B)	0.65	T
14	Total number of Permanent magnet	10	-
15	Total number of pairs of stator slot and tooth	24	-
16	Total number of coil	12	-
17	Total number of turns of the coil	528	turns
18	Number of pole	4	-
19	Total length of the coil	147	m
20	Energy product of the permanent magnet	168.2	KJ/m^3
21	Strength of the electromagnetic field	2.6×10^5	A/m

Design of the proposed EMC system starts with analytical calculation results from equation 3.11. The result showed that magnitude of electromagnetic force required to couple rotor and armature plate of the EMC system is 7.2 KN. Then a theory and sizing equation that can express components of the required electromagnetic force are applied to equivalent electromagnetic circuit model of the EMC system shown in figure 3.7. Equation 3.1 showed that the required electromagnetic force is a factor of magnitude of electromagnetic flux density induced and effective cross sectional area of the EMC system. According to this analysis; electromagnetic flux density of 0.65 T is determined to achieve electromagnetic force of 7.2 KN and it is assumed to be equally distributed over the effective cross sectional area of 0.036 m^2.But equation 3.2 showed that magnitude of the electromagnetic field density is influenced by factors such as, length of the air gap, number of turns of the coil and geometric dimensions of the EMC system.

However, it could be noted that when the air gap decreases, electromagnetic field density is expected to increase and allow less space for windings, but also the reluctance of the main flux path increase (Neil Lovell Brown, 2002). The objective of this design optimization part is to determine the optimum value of the air gap length that can allow high electromagnetic field density and low reluctance for the proposed EMC system. Analytical calculation results from equation 3.5 showed that the effective total length of the air gap required to pass the electromagnetic field is 0.033m. Another component of the electromagnetic force that should be determined is, number of turns of coil required to induce the electromagnetic flux density of 0.65T in the defined air gap length of 0.033m.Analytical calculation results from equation 3.2 showed that 528 number of turns of coil are required.

Thus, based on analytical calculation results obtained from the equivalent electromagnetic circuit model, optimum geometric dimensions of stator should be determined. Choice of suitable stator topology and winding type is the basis for the design optimizations of physical dimension of the EMC system (Kevin .S, 2017). To achieve this goal, comparison between different stator arrangement and winding type was discussed in section 3.7.3. Double flux axial stator has been chosen as interesting topology .Because this stator brings advantage such as; two working surface allowing more electromagnetic flux density to be developed, smaller volume to fit the existing bell house, less loose and simple maintenance. Based on this analysis, the basic topology of the electromagnetic clutch had been developed as shown in figure 3.13 and sizing equation was explored to calculate axial length of the rotor, stator and armature plate. Analytical calculation results from equation 3.15 showed that total axial length required for stator slot in both side is 45.4 mm. This is provided to hold total number of turns of the coil. Analytical calculation result from equation 3.17 showed that axial length the stator core is 56.6mm. Similarly sizing equation for axial length was applied to rotor. Analytical calculation results from equation 3.18 and 3.20 show that optimum axial length for rotor is 32.2mm and it was found that armature plate has the axial length with the rotor. However, from equation 3.31 it could be noted that axial length of permanent magnet is influenced by the air gap length .Analytical calculation result showed permanent magnet with axial length of 4.4 mm is required for the defined air gap length. Usually permanent magnets are required to reduce flux leakage and permit to concentrate the electromagnetic flux density in the air gaps. Therefore it proves that we can find that almost all electromagnetic flux pass through the air gaps of constant effective cross sectional area (Samuel , 2006). Choice of the permanent magnet materials are mainly depends on their operating energy product, which is the product of the magnitude electromagnetic field density and field strength in the air gap (BH).Analytical calculation result showed that permanent magnet with attainable energy product of 168.2 KJ/m^3 is required. Based on the energy product comparison of the permanent magnet materials listed on table 3.3, it was found that Samarium-Cobalt (SmCo) permanent magnet material has good performance to concentrate the electromagnetic field density of 0.65 T. However, equation 3.27 showed that the optimum number of the permanent magnet required is expressed as a function of number of stator slot per one stator winding and number of phase of the winding. Therefore, comparison between different winding types was carried out in section 3.7.3.The comparison result showed that chose of toroidal winding layout is interesting for the EMC system application. Because it brings advantage such as; winding length can be made very short, this can allow maximizing the limited space for the EMC system. This winding type has features such as; 12 number of stator winding, 2 numbers of stator slots per one stator winding, 4 pole and 3 phase of stator winding. Then analytical calculation result from equation 3.27 showed that 10 numbers of the permanent magnets are required for each rotor and armature plate. Moreover, optimum geometric dimensions of the permanent magnet should be determined to fit circumferential face of the rotor and armature plate. In this optimization process, the direct decent method is used. This means that the inner and outer diameter of the rotor and armature plate is 175 mm and 275 mm respectively. Generally there exist the relationship between the given dimension and objective function related to geometric dimension of the permanent magnet. Based on the inner and outer circumference of the rotor and armature plate, analytical calculation result from equation 3.30 and 3.31 showed that top width and bottom width of the permanent magnet on the surface of the rotor are 56.2 mm and 28.3 mm respectively. Analytical calculation result from equation 3.32 showed that slot width of the permanent magnets is 26.6mm.It was found that permanent magnet on the surface of rotor and armature plate has geometric dimensions.

Finally, the analytical calculation result has shown that the proposed electromagnetic clutch system provides reduction of axial length of the existing bell house by 30.3 mm and the number of clutch components is reduced from 5 to 3. This results showed good agreement with the effectiveness of the EMC system .Therefore, the EMC system can be used for future manual transmission drive systems not only for Toyota 3L but also for other applications where clutches are being used.

CHAPTER FIVE

5. CONCLUSSION AND RECOMMENDATION

5.1. Summary

This section presents the multi disciplinary design and analysis methods for this thesis work. All the design and analysis methods are discussed in terms of two major parts of the thesis work, namely electromagnetic part and mechanical parts. In the design of electromagnetic parts, analytical modeling method was generally accepted as a method for computing the electromagnetic circuit properties. Such method lies in sectioning the geometry of the electromagnetic cutch system and applying 2D electromagnetic field analysis and allowing the exploration of the electromagnetic field distribution and field quantities of the complex assembly of the electromagnetic clutch system. In the design of mechanical parts, dimension and performance parameters are calculated corresponding to assumed design limitations. Several investigations in previous work have been presented to show effectiveness of the proposed design and analysis methods.

5.2 Conclusion

This thesis has focused on the design of EMC system for Toyota 3L, manual transmission. Based on the results obtained the following conclusions are drawn:

- The design and analysis has shown that the proposed electromagnetic clutch system provides reduction of axial length of the existing bell house by 30.3 mm and the number of clutch components are reduced from 5 to 3.
- The analysis has shown that the proposed electromagnetic clutch system can fit bell house of the existing clutch system.
- The electromagnetic clutch system is capable to transmit mechanical torque between engine and gear box of Toyota 3L, manual transmission.
- Components of the electromagnetic clutch system such as; rotor, double face axial stator and armature plate can replace components of the existing clutch system such as; friction disc, pressure plate, diaphragm spring and release bearing with its complex hydraulic actuation mechanism.
- There are no mechanically contacting parts in the proposed electromagnetic clutch system. Therefore, the proposed EMC system offer solution for wear and slip problem of the existing clutch system and it has long service life with minimum maintenance requirements compared with the existing one.

5.3 Recommendation

Given the time frame and the resources available, this thesis work establishes a theoretical base and analytical calculation for the design of the proposed electromagnetic clutch system.

On the basis of the present thesis work, some recommendations for ASTU are drawn as follows:

- It would be interesting for teaching purpose, if model of the EMC system is installed physically in the automotive power train shop. It is clear that in this model automotive engineering students would have to keep close watch on its operation and design conditions, in order to detect any remaining design requirements and develop the EMC system.
- Another point is that further development and investigation should be carried out in order to gain more understanding regarding the change in accuracy and effects of heating on the EMC system. Thus, interested ASTU staff may conduct further study and controlled experiment on the EMC system using professional search from electrical engineering department.

5.4 Future work

The most important work that must be done for the EMC system is to develop a test stand and record meaningful data that can be analyzed to understand its behavior operating region. Finally, it is important to characterize the non-linearities and irregularities in the EMC system at very low load and low voltage operating points.

References

[1] Asghar.S and Gholamian. (2001).Optimum Design of Slotted Axial Flux Internal Stator Motor Using Genetic Algorithm for Electric Vehicle. International Journal of Software Engineering & Applications (IJSEA), Vol.2.

[2] Athani, A., Rama, N., H.M., Somaya, N., & Sridhar, N. (2016, May). Design and working of electromagnetic clutch to reduce wear and slip. International Journal of Current Trends in Engineering & Research, Volume 2, pp. 202 – 21.

[3] Baiba, L. (2015**).** Design optimization of cylindrical magnetic coupler based on calculations of magnetic field, Unpublished Ph.D.Thesis submitted to Riga technical university, 41pp.

[4] Bertoluzzo, M., & Buja, G. (2011). Development of electric propulsion systems for light electric vehicles. IEEE Transactions on Industrial Informatics, *7*(3), 428-435.

[5] Bezzazi, M., Khamlichi, A., Jabbouri, A., Reis, P., & Davim, J. P. (2007). Experimental characterization of frictional behavior of clutch facings using Pin-on-disk machine. Materials & design, *28*(7), 2148-2153.

[6] Bodine. (2001) .Small Motor, Gear motor and control. Hand book. Fifth edition, 210p.

[7] Charles. (2010). Solenoids Electromagnets and Electromagnetic windings, 46p.

[8] Dieter, G. E. (2000).Engineering Design. Third Edition, 67p.

[9] Dym. L & Little, P. (2000). Engineering design: a project-based approach, 256p.

[10] Eljaroshi, E. (2014).The modeling, Design and the operation of An Electromagnetic torque converter, Unpublished Ph.D.Thesis submitted to Leicester University.

[11] Francesco, B., Paola, F., Frendo, Bingli, Z., & Qingliang, H., (2015) .Temperature, Effect on the Torque Characteristic of a Magneto rheological Clutch. Proc of ELSEVIER, IntellindSyst, pp23-26.

[12] Gao, A., Chen, H,. Liu, Q., &Chu, Q. (2002).Friction characteristics of a paper-based friction material. Int. J. Automotive Tech., 3, (4), pp. 171-176 .

[13] Gavril &V. Ionita. (2002, June). Crystalline and amorphous soft magnetic materials and their applications status of art and challenges. Journal of electronics and Advanced Materials, Vol. 4, No. 2, p. 173 – 192

[14] Gupta. (2005).Text book of machine design. First edition.

[15] Hansel man, D. (2003). Brushless Permanent Magnet Motor Design. New York: Elsevier Scientific Publishing Company, p 330.

[16] Hao. G. & Marco Ceccarelli. (2012). A multy objective optimal path planning for 1- DOF clutched *ARM* .Proc of ELSEVIER, vol. 3, no. 5,pp 40:1,109-121

[17] Jack Erjavec. (2009).Automotive technology system approach. 5th edition, 678p.

[18] Jessy cussack. (2013) .Design of a High Speed Clutch with Mechanical Pulse-Width Control, Unpublished M.Sc. Thesis submitted to Worcester polytechnic institute.

[19] Jiangchuan, L., Feng, D., Shaojin, L., & Hoa, H. (2013). Analysis of the Influence of Clutch Pedal to Vehicle Comfort. Automotive Congress, Lecture Notes in Electrical Engineering.

[20] Jiang Kejun, Heren & Zhanglanchun. (2015).Application and Control Method of Electromagnetic Synchronizer for Double Rotor Motor Power Coupling System. Electronics, vol. 19, no. 2, pp.88-93.

[21] Jindle. M. (2015).Identification and position control of electromagnetic clutch. Proc of ELSEVIER, pp.11-053–058.

[22] Kastinger .G. (1998).Analysis of Torque Computation of a Toroidal-Coil-Motor by Finite Element Method. PCIM'98 Intelligent Motion.

[23] Kaliyev. (2015). Axial Flux Permanent Magnet Coreless Machine, Unpublished Bachelor of Electrical and electronics engineering .Thesis submitted to University of southern Queensland, 35p.

[24] Lathiya, N., Badola, C., Undhad & Dhamecha, B. (2014).A Literature Review on Failure in Single Plate Clutch System. International Journal for Scientific Research & Development, Vol. 2, Issue 10, 2014.

[25] Martin Kirchengast, Martin Steinberger, Daniel prix & Martin Horn. (2015).Identification and position control of electromagnetic clutch, Proc of ELSEVIER, pp.11-053–058.

[26] Martin, S., & Jacob, R. (2015). Observe design for an electromagnetically actuated dry clutch. Proc of ELSEVIER, pp 69-72.

[27] M. Eguchi, M., Takei & T. Yamamoto. (2005).Shear characteristics of a boundary film for a paper-based wet friction material: friction and real contact area measurement. Trib. Int., 38, pp. 327-335.

[28] Mahmoudi, N.A.Rahim & Kahourzade. (2013, April). Design, Analysis and Prototyping of an axial-flux Permanent magnet Motor Based on Genetic Algorithm and Finite-Element Analysis. IEEE transactions on magnetic, vol.49.

[29] Namrata .A.N & Prof.Dheeraj.V. (2016) .Analysis of 23 Degree Inclined Grooves Made on Dry Friction Clutch. International Journal of Innovative Research in Science, Engineering and Technology, Vol. 5.

[30] Nicola Cappetti, Mario Pisaturo & Adolfo Senatore. (2012).Modeling the cushion spring characteristic to enhance the automated dry-clutch performance: The temperature effect. Journal of Automobile Engineering, 226(11):1472–1482.

[31] Neil Lovell & Brown. (2002). Compact Electrical Generators for Diesel Driven Generating Sets. Durham University.

[32] Pahl, G., Beitz, W., Feldhusein, J., & Grote, K. (2007).Engineering Design: A Systematic Approach. Third Edition, London.

[33] Potluri, P., Kusak, E., & Reddy, T. (2003) .Novel stitch bonded sandwich composite structures. Composite structures, 59, 251-259.

[34] Prof.K.P.Kattimani,Raviraj,A.,Shewate,Rohit,M.,Supe,Mukund,C.,&Sonawane.(2018).Transmission Braking System by Using Electromagnetic Clutch-ISSN: 2278-1684, p-ISSN: 2320-334X, PP. 24-29.

[35] Ravibala.S, Dr.SS Chauhan & Ass.Prof.Ranjeet Kumar. (2016). Review on friction clutch Plate of an ATV. International Journal of Advance Engineering and Research Development Volume 3.

[36] Rico, B. (2012) .New Energy-Efficient Electromagnetic Clutch for Automotive Air Conditioning Compressors. International Refrigeration and Air Conditioning Conference.

[37] Rhythm, D., Sanket, G., Nitish, K., & Jarti. (2016).Design & Theoretical Study of Electromagnetic Braking System. e-ISSN: 2278-1684,p-ISSN: 2320-334X, Volume 13, Issue 6 Ver., PP 87-96

[38] Riviera. J& Myrna, S. (2009). Handbook of surface and interface analysis: methods for problem-solving. CRC press.

[39] Robert W.Erickson. (2001) .Fundamentals of Power Electronics. Second Edition, Academic Publishers, New York.

[40] S.Sanda, Y.Nagasawa, A. Suzuki, K.Hayashi & H. Itoh. (1995) .Mechanism of friction of wet clutch with paper based facings. Part 1 Observation and modeling of facing surface during engagement. Proc. Int. Trib. Conf, pp 1519 - 1524.

[41] Samuel. (2006).Comparative study and selection criteria of linear motors.

[42] Sahin, F. (2001). Design and development of a high-speed axial-flux permanent-magnet machine. Technical college of Eindhoven.

[43] Theraja, B. (2005).A Text book of electrical technology (first edition). volume1, 610p.

[44] Tomasz. H & Krzysztof.F. (2009).Modeling of Magnetic Attraction Force of Electromagnetic Module in a Relative Base – Air-gap – Absolute Base System. Solid State Phenomena ,Vol. 144 (2009), pp 53-58

[45] Vahid Manhattan. (2013).Design and Development of an Actuation System for the Synchronized Segmentally Interchanging Pulley Transmission System, Unpublished Ph.D.Thesis submitted to University of Toronto, 34p.

[46] Wanli, (2011).Analysis and design of permanent magnet bi-stable electromagnetic Clutch unit for in wheel electric vehicle drives. ISSN 1996-1073.

[47] Werner Eduardo. (2016, October).Axial Flux Permanent Magnet Machines – Development of Optimal Design Strategies. ISBN 978-952-335-024-3.

[48] Yuan and Wan. (2017).Electromagnetic Design and Losses Analysis of a High-Speed Permanent Magnet Synchronous Motor with Toroidal Windings for Pulsed Alternator. IEEE Trans, vol. 61, no. 6, pp. 2946-2959.

[49] Zhang, Z. (2018, September). Design and Multi-physical Fields Analysis of High Speed Permanent Magnet, Unpublished Ph.D.Thesis submitted to the Queen’s University.

Appendix

All dimensions are given in terms of mm.

2D of the rotor

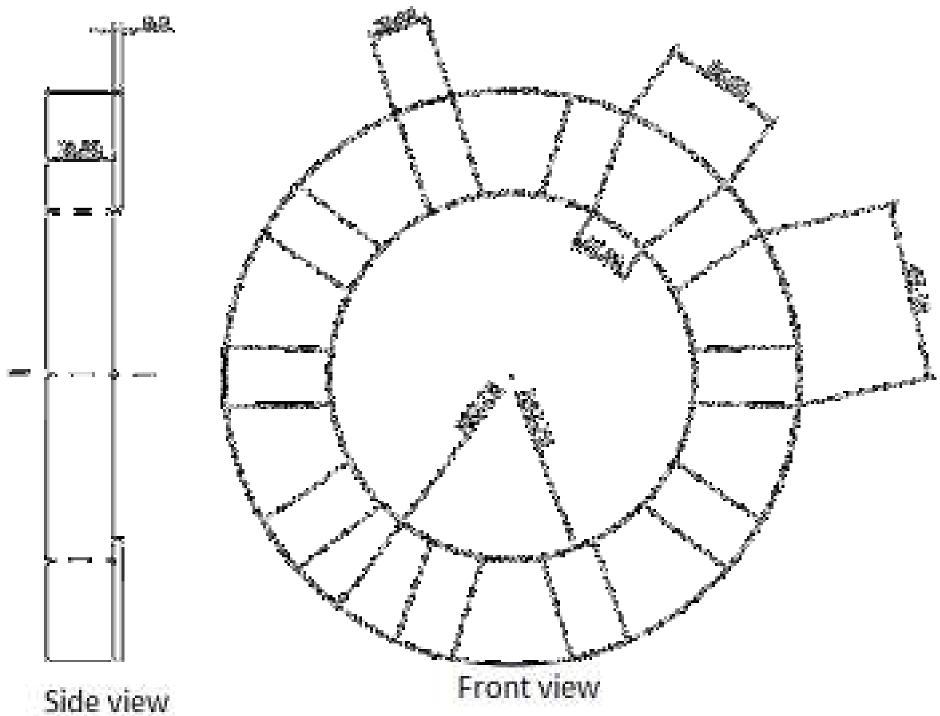

2D of the Stator

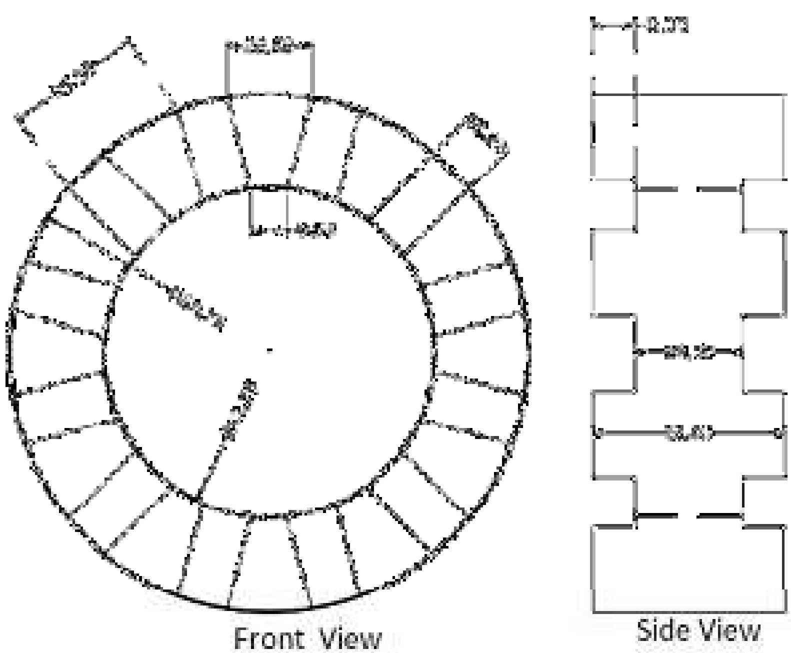

2D of the Armature plate